การสังเคราะห์และสมบัติของสารประกอบเชิงซ้อนโลหะชิฟเบสจาก เอมีนและอนุพันธ์ซาลิซิลัลดีไฮด์

นายหัสษดี เดชเสน

วิทยานิพนธ์นี้เป็นส่วนหนึ่งของการศึกษาตามหลักสูตรปริญญาวิทยาศาสตรมหาบัณฑิต
สาขาวิชาเคมี ภาควิชาเคมี
คณะวิทยาศาสตร์ จุฬาลงกรณ์มหาวิทยาลัย
ปีการศึกษา 2547
ISBN 974-17-6473-1

SYNTHESIS AND PROPERTIES OF SCHIFF BASE METAL COMPLEXES FROM AMINE AND SALICYLALDEHYDE DERIVATIVES

Mr. Hussadee Detsen

A Thesis Submitted in Partial Fulfillment of the Requirements
for the Degree of Master of Science in Chemistry
Department of Chemistry
Faculty of Science
Chulalongkorn University
Academic Year 2004

ISBN 974-17-6473-1

Thesis title	SYNTHESIS AND PROPERTIES OF SCHIFF BASE METAL COMPLEXES FROM AMINE AND SALICYLALDEHYDE DERIVATIVES
By	Mr. Hussadee Detsen
Field of study	Chemistry
Thesis Advisor	Associate Professor Nuanphun Chantarasiri, Ph.D.
Thesis Co-advisor	Associate Professor Vithaya Ruangpornvisuti, Ph.D.

Accepted by the Faculty of Science, Chulalongkorn University in Partial Fulfillment of the Requirements for the Master's Degree

……...Dean of the Faculty of Science
(Professor Piamsak Menasveta, Ph.D.)

Thesis committee

……...Chairman
(Professor Udom Kokphol, Ph.D.)

……Thesis Advisor
(Associate Professor Nuanphun Chantarasiri, Ph.D.)

……Thesis Co-advisor
(Associate Professor Vithaya Ruangpornvisuti, Ph.D.)

…….Member
(Assistant Professor Thawatchai Tuntulani, Ph.D.)

…….Member
(Assistant Professor Polkit Sangvanich, Ph.D.)

หัสษดี เดชเสน : การสังเคราะห์และสมบัติของสารประกอบเชิงซ้อนโลหะชิฟเบสจากเอมีนและอนุพันธ์ซาลิซิลัลดีไฮด์. (SYNTHESIS AND PROPERTIES OF SCHIFF BASE METAL COMPLEXES FROM AMINE AND SALICYLALDEHYDE DERIVATIVES อ.ที่ปรึกษา : รศ.ดร.นวลพรรณ จันทรศิริ; อ.ที่ปรึกษาร่วม : รศ.ดร.วิทยา เรืองพรวิสุทธิ์; 70 หน้า, ISBN 974-17-6473-1.

สารประกอบเชิงซ้อนเฮกซาเดนเทตชิฟเบสของโลหะสังกะสีและโลหะนิกเกิลถูกสังเคราะห์จากปฏิกิริยาระหว่างซาลิซิลัลดีไฮด์หรืออนุพันธ์ของซาลิซิลัลดีไฮด์, โลหะแอซิเทต และไตรเอทิลีนเททระเอมีนในอัตราส่วนโมล 2:1:1 ค่าคงที่การเกิดโปรโตเนชันของ Sal_2trien, $Sal_2(OMe)trien$, $Sal_2(OEt)trien$ และค่าคงที่ความเสถียรของสารประกอบเชิงซ้อน หาได้จากการทดลองโดยวิธีโพเทนชิโอเมทริกไทเทชันในสารละลายเตตระแอมโมเนียม ไตรฟลูออโรมีเทนซัลโฟเนตเข้มข้น 1.0×10^{-2} โมลาร์ ในตัวทำละลายเมทานอลที่อุณหภูมิ 25 องศาเซลเซียส ค่าคงที่ความเสถียรการเกิดสารประกอบเชิงซ้อนของ $ZnSal_2trien$, $ZnSal_2(OMe)trien$ และ $ZnSal_2(OEt)trien$ ในเทอมของ log β มีค่าเท่ากับ 4.56 ± 0.05, 4.30 ± 0.11, 3.76 ± 0.09 ตามลำดับ และค่าความเสถียรของการเกิดสารประกอบเชิงซ้อน $NiSal_2trien$, $NiSal_2(OMe)trien$ และ $NiSal_2(OEt)trien$ มีค่าเท่ากับ 4.80 ± 0.17, 5.77 ± 0.14, 7.08 ± 0.03 ตามลำดับ ค่าคงที่ความเสถียรของสารประกอบเชิงซ้อนของนิกเกิลมีค่าสูงกว่าสารประกอบเชิงซ้อนของสังกะสี ซึ่งแสดงให้เห็นว่าสารประกอบเชิงซ้อนของนิกเกิลมีความเสถียรกว่าสารประกอบเชิงซ้อนของสังกะสี ผลการทดลองนี้สอดคล้องกับอนุกรมของ Irving และ William ซึ่งอธิบายลำดับความเสถียรของสารประกอบเชิงซ้อนของโลหะต่างๆคือ $Cu^{2+} > Ni^{2+} > Zn^{2+}$ โครงสร้างของ Sal_2trien, $Sal_2(OMe)trien$, $Sal_2(OEt)trien$, $ZnSal_2trien$, $ZnSal_2(OMe)trien$ และ $ZnSal_2(OEt)trien$ คำนวณโดยใช้ทฤษฎีเดนซิตีฟังก์ชันที่ระดับ 6-31G(d) เป็นเบสิสเซต พลังงานทางเทอร์โมไดนามิกส์ของ Sal_2trien, $Sal_2(OMe)trien$, $Sal_2(OEt)trien$, $ZnSal_2trien$, $ZnSal_2(OMe)trien$ และ $ZnSal_2(OEt)trien$ คำนวณโดยทฤษฎีระดับ 6-31G(d)

ภาควิชา เคมี ลายมือชื่อนิสิต.....

สาขาวิชา เคมี ลายมือชื่ออาจารย์ที่ปรึกษา.....

ปีการศึกษา 2547 ลายมือชื่ออาจารย์ที่ปรึกษาร่วม.....

4572562823: MAJOR CHEMISTRY
KEYWORD: HEXADENTATE SCHIFF BASE METAL COMPLEXES, PROTONATION CONSTANT, STABILITY CONSTANT, DENSITY FUNCTIONAL THEORY

HUSSADEE DETSEN: SYNTHESIS AND PROPERTIES OF SCHIFF BASE METAL COMPLEXES FROM AMINE AND SALICYLALDEHYDE DERIVATIVES. THESIS ADVISOR: ASSOC. PROF. NUANPHUN CHANTARASIRI, Ph.D. THESIS CO-ADVISOR: ASSOC. PROF. VITHAYA RUANGPORNVISUTI, Ph.D. 70 pp. ISBN 974-17-6473-1

Hexadentate Schiff base zinc(II) and nickel(II) complexes were synthesized from the reaction between salicylaldehyde or salicylaldehyde derivatives, metal (II) acetate and triethylenetetramine at the mol ratio of 2:1:1. Protonation constants of Sal_2trien, Sal_2(OMe)trien, Sal_2(OEt)trien and stability constants of their zinc and nickel complexes were determined by potentiometric titration technique using 1.00 x 10^{-2} M $Bu_4NCF_3SO_3$ in methanol at 25 ^oC. Stability constants in term log β are 4.56 ± 0.05, 4.30 ± 0.11, 3.76 ± 0.09 for $ZnSal_2$trien, $ZnSal_2$(OMe)trien, $ZnSal_2$(OEt)trien and 4.80 ± 0.17, 5.77 ± 0.14, 7.08 ± 0.03 for $NiSal_2$trien, $NiSal_2$(OMe)trien, $NiSal_2$(OEt)trien, respectively. The stability constants of nickel complexes are higher than those zinc complexes which indicates that nickel complexes are more stable than zinc complexes. This result corresponds to the Irving-William sequence, which describes that the order of stability constant for metal complexes from different cation is $Cu^{2+} > Ni^{2+} > Zn^{2+}$. The structures of Sal_2trien, Sal_2(OMe)trien, Sal_2(OEt)trien, $ZnSal_2$trien, $ZnSal_2$(OMe)trien and $ZnSal_2$(OEt)trien were optimized by Density Functional Theory (DFT) calculation using 6-31G(d) basis set. Total of thermodynamic energies of Sal_2trien, Sal_2(OMe)trien, Sal_2(OEt)trien and their zinc complexes were computed at B3LYP/6-31G(d) level of theory.

Department……Chemistry…….. Student's signature……..
Field of study……Chemistry…… Advisor's signature……..
Academic year……2004…….. Co-advisor's signature…….

ACKNOWLEDGEMENTS

I wish to express the highest appreciation to my thesis advisor, Assoc. Prof. Dr. Nuanphun Chantarasiri, and my thesis co-advisor, Assoc. Prof. Dr. Vithaya Ruangpornvisuti, for their suggestion, profound assistance, encouragement, dedication, kindness and especially sincere forgiveness for my harsh mistakes throughout my master degree career. In addition, I would like to thank and pay my respect to Prof. Dr. Udom Kokpol, Assist. Prof. Dr. Thawatchai Tuntulani and Assist. Prof. Dr. Polkit Sangvanich for their valuable suggestions and comments as committee members and thesis examiners.

This thesis cannot be completed without kindness and helps of many people. First, I am grateful to the Thailand Research Fund, Chulalongkorn University Radchadaphisek Somphot Grant and Graduate School of Chulalongkorn University for financial support of this research. Then, I wish to thank all former and present staff in Supramolecular Chemistry Research Unit especially Mr. Banchob Wanno for valuable suggestions. Special thanks are due to Assistant Professor Dr. Narongsak Chaichit, Department of physics, Faculty of Science and Technology, Thammasat University, Assistant Professor Dr. Chaweng Pakawatchai, Department of Chemistry, Faculty of Science, Prince of Songkhla University and Assistant Professor Dr. Nongnuj Muangsin, Department of Chemistry, Faculty of Science, Chulalongkorn University for X-ray crystallography.

Finally, I would like to express my deepest gratitude to my family, especially my father and my mother for their kindness, encouragement, financial supports and important assistance throughout my life. I would like to thank to my sister, Miss Jaruwan Detsen, for love, care and financial support throughout my graduate study.

CONTENTS

Page

Abstract in Thai…….. iv

Abstract in English……. v

Acknowledgements…… vi

Contents…….. vii

List of Figures……. xi

List of Tables…….. xiii

List of Schemes……... xv

List of Symbols and Abbreviations…… xvi

CHAPTER I INTRODUCTION…… 1

1.1 Schiff base metal complexes…….. 1

1.2 Measurement of protonation constants and stability constants…….. 4

1.3 Quantum chemical calculation……... 8

1.4 Objective and scope of this thesis…….. 9

CHAPTER II THEORY…….. 10

2.1 Chemical equilibrium and potentiometry…… 10

2.1.1 Concentration constants and activity constants……... 10

2.1.2 Protonation constants……... 12

2.1.3 Stability constants…… 13

2.1.4 Secondary concentration variables…….. 15

2.1.4.1 The protonation formationfunction $(\bar{P})$ …….. 15

2.1.4.2 The complex formation function $(\bar{n})$ …….. 16

2.1.5 Computation of equilibrium constants by SUPERQUAD program…… 18

CONTENTS (CONTINUED)

Page

2.2 Quantum chemical calculation…… 20

2.2.1 Basis set effects……... 20

2.2.1.1 Minimal basis sets……... 20

2.2.1.2 Split valence basis sets…… 21

2.2.1.3 Practical considerations when performing ab initio calculations…… 21

2.2.1.4 Setting up the calculation and choice of coordinates.. 22

2.2.1.5 Calculating derivatives of the energy……. 22

CHAPTER III EXPERIMENTAL…… 23

3.1 Materials……. 23

3.2 Analytical Procedures……. 23

3.3 Synthetic Procedure…… 23

3.3.1 Synthesis of hexadentate Schiff base zinc complexes…… 24

3.3.1.1 Preparation of bis(salicylaldiminato)triethylenetetramine zinc(II) complex [$ZnSal_2$trien]……. 24

3.3.1.2 Preparation of bis(3-methoxysalicylaldiminato) triethylenetetramine zinc(II) complex [$ZnSal_2$(OMe)trien]…… 24

3.3.1.3 Preparation of bis(3-ethoxysalicylaldiminato) triethylenetetramine zinc(II) complex [$ZnSal_2$(OEt)trien]…… 25

3.3.1.4 Preparation of bis(3,5-di-*tert*-butyl-salicylaldiminato) triethylene tetramine zinc(II) complex [$ZnSal_2$(di-*t*-Bu)trien]…….. 25

3.3.2 Synthesis of hexadentate Schiff base nickel complexes……. 26

3.3.2.1 Preparation of bis(salicylaldiminato)triethylenetetra mine nickel(II) complex [$NiSal_2$trien]……... 26

CONTENTS (CONTINUED)

Page

3.3.2.2 Preparation of bis(3-methoxysalicylaldiminato) triethylenetetramine nickel(II) complex[$NiSal_2$(OMe) trien]…… 26

3.3.2.3 Preparation of bis(3-ethoxysalicylaldiminato) triethylenetetramine nickel(II) complex [$NiSal_2$(OEt) trien]…… 27

3.3.2.4 Preparation of bis(3,5-di-*tert*-butyl-salicylaldiminato) triethylene tetramine nickel(II) complex [$NiSal_2$(di-*t*-Bu)trien]…….. 27

3.4 Potentiometric measurements……. 28

3.5 Quantum chemical calculations…….. 31

CHAPTER IV RESULTS AND DISCUSSION…… 33

4.1 Synthesis of hexadentate Schiff base metal complexes……. 33

4.2 Protonation constants by potentiometric measurements……..... 35

4.3 Hexadentate Schiff base zinc complexes…… 38

4.3.1 $ZnSal_2$trien…….. 38

4.3.2 $ZnSal_2$(OMe)trien……... 41

4.3.3 $ZnSal_2$(OEt)trien……. 42

4.4 Hexadentate Schiff base nickel complexes…… 43

4.4.1 $NiSal_2$trien…….. 43

4.4.2 $NiSal_2$(OMe)trien……... 45

4.4.3 $NiSal_2$(OEt)trien……. 46

4.5 Stability constants by potentiometric measurements…….. 48

4.6 Quantum chemical calculations…….. 50

CHAPTER V CONCLUSION…… 63

CONTENTS (CONTINUED)

Page

REFERENCES…….. 65

VITAE…… 70

LIST OF FIGURES

Page

Figure 1.1	Structure of manganese-salen complexes……	2
Figure 1.2	Structure of *N*-*N*′-bis-(4-dimethylamino-benzylidine)-benzene-1,2-diamine……..	3
Figure 1.3	Structure of unsymmetrical isomers (2-pyridylmethyl, 3-pyridylmethyl) amine……...	6
Figure 1.4	Geometry-optimized structure for monomeric zwitterion and 2-benzyliminomethylene-4-nitrophenol……..	9
Figure 4.1	X-ray crystal structure of $ZnSal_2$trien……..	34
Figure 4.2	X-ray crystal structure of $ZnSal_2$(OMe)trien……...	35
Figure 4.3	Species distribution plot of Sal_2trien (L^{2-}) and $ZnSal_2$trien (ZnL) in 1.0 x 10^{-2} M $Bu_4NCF_3SO_3$ in methanol at 25 ^oC, C_{ZnL} = 7.685 x 10^{-4} M…….....	39
Figure 4.4	Species distribution plot of Sal_2(OMe)trien (L^{2-}) and $ZnSal_2$(OMe) trien (ZnL) in 1.00 x 10^{-2} M $Bu_4NCF_3SO_3$ in methanol at 25 ^oC, C_{ZnL} = 8.325 x 10^{-4} M……	41
Figure 4.5	Species distribution plot of Sal_2(OEt)trien (L^{2-}) and $ZnSal_2$(OEt) trien (ZnL) in 1.00 x 10^{-2} M $Bu_4NCF_3SO_3$ in methanol at 25 ^oC, C_{ZnL} = 9.091 x 10^{-4} M……	43
Figure 4.6	Species distribution plot of Sal_2trien (L^{2-}) and $NiSal_2$trien (NiL) in 1.00 x 10^{-2} M $Bu_4NCF_3SO_3$ in methanol at 25 ^oC, C_{NiL} = 9.505 x 10^{-4} M……...	44
Figure 4.7	Species distribution plot of Sal_2(OMe)trien (L^{2-}) and $NiSal_2$(OMe) trien (NiL) in 1.00 x 10^{-2} M $Bu_4NCF_3SO_3$ in methanol at 25 ^oC, C_{NiL} = 8.317 x 10^{-4} M……..	45
Figure 4.8	Species distribution plot of Sal_2(OEt)trien (L^{2-}) and $NiSal_2$(OEt) trien (NiL) in 1.00 x 10^{-2} M $Bu_4NCF_3SO_3$ in methanol at 25 ^oC, C_{NiL} = 8.333 x 10^{-4} M……..	47
Figure 4.9	Titration curve of 9.081 x 10^{-4} M $NiSal_2$(di-*t*-Bu)trien with 5.00 x 10^{-2} M tetrabutylammonium hydroxide…….	48

LIST OF FIGURES (CONTINUED)

Page

Figure 4.10 B3LYP/6-31G(d)-optimized structures of (a) free form, (b) complex form of Sal_2trien, (c) free form and (d) complex form of Sal_2(OMe)trien, (e) free form and (f) complex form of Sal_2(OEt)trien. 54

LIST OF TABLES

Page

Table 1.1	Asymmetric epoxidation of *cis*-β-Methylstyrene with catalysis 1-5..	2
Table 1.2	Log *K* values for the stability constants of the mononuclear and homodinuclear complexes of BDBPH (μ = 0.10 M (KCl), 25 ^{o}C, under argon)……	6
Table 1.3	Acidity constants of unsymmetrical isomers (2-pyridylmethyl, 3-pyridylmethyl) amine……..	7
Table 1.4	Stability constants of copper(II) complexes ……	8
Table 3.1	Experimental data for determining the protonation constants and stability constants of zinc complexes…….	29
Table 3.2	Experimental data for determining the protonation constants and stability constants of nickel complexes……..	30
Table 4.1	Protonation constants of Sal_2trien, (L^{2-})…….	38
Table 4.2	Atomic charges of binding atoms in free forms of Sal_2trien, Sal_2(OMe)trien, Sal_2(OEt)trien and their complexing forms with Zn^{2+} ion…….	40
Table 4.3	Protonation constants of Sal_2(OMe)trien, (L^{2-})…….	41
Table 4.4	Protonation constants of Sal_2(OEt)trien, (L^{2-})……...	42
Table 4.5	Protonation constants of Sal_2trien, (L^{2-})……	44
Table 4.6	Protonation constants of Sal_2(OMe)trien, (L^{2-})…….	45
Table 4.7	Protonation constants of Sal_2(OEt)trien, (L^{2-})……...	46
Table 4.8	Stability constants of zinc and nickel complexes in 1.00 x 10^{-2} M $Bu_4NCF_3SO_3$ in methanol at 25 ^{o}C…….	49
Table 4.9	Stability constants for 1,2,3-triaminopropane and *N*-(2-aminoethyl) ethylenediamine complexes of transition metals (measured at 20 ^{o}C in an aqueous medium 0.1 M in KCl)……	49
Table 4.10	Physical properties of elements nickel and zinc……	50
Table 4.11	Total energies and thermodynamic quantities of Sal_2trien, Sal_2(OMe) trien, Sal_2(OEt)trien and their Zinc complexes were computed at B3LYP/6-31G(d) level of theory……	51

LIST OF TABLES (CONTINUED)

Page

Table 4.12 Preorganization energies of Sal_2trien, binding and complexation energies of zinc complexes were computed at B3LYP/6-31G(d) level of theory……. 52

Table 4.13 Preorganization energies of Sal_2(OMe)trien, binding and complexation energies of zinc complexes were computed at B3LYP/6-31G(d) level of theory…… 52

Table 4.14 Preorganization energies of Sal_2(OEt)trien, binding and complexation energies of zinc complexes were computed at B3LYP/6-31G(d) level of theory…… 53

Table 4.15 Hydrogen bond distance between phenolate oxygen ion and hydrogen atom of secondary amine of Schiff base ligands…… 53

Table 4.16 Bond length data for the structures of $ZnSal_2$trien, $ZnSal_2$(OMe)trien and $ZnSal_2$(OEt)trien…….. 58

Table 4.17 Bond angles data for the structures of $ZnSal_2$trien, $ZnSal_2$(OMe)trien and $ZnSal_2$(OEt)trien…….. 60

Table 4.18 Dihedral angles data for the structures of $ZnSal_2$trien, $ZnSal_2$(OMe) trien and $ZnSal_2$(OEt)trien…….. 62

LIST OF SCHEMES

Page

Scheme 1.1	Synthesis of imines……..	1
Scheme 1.2	Synthesis of metal-containing epoxy polymers from DEGBA and hexadentate Schiff base metal complexes…….	3
Scheme 1.3	Synthesis of metal-containing polyureas from the reaction between metal complexes and diisocyanates……..	4
Scheme 1.4	Synthesis of BDBPH……	5
Scheme 1.5	Synthesis of hexadentate Schiff base metal complexes……...	10
Scheme 4.1	Synthesis of Schiff base metal complexes……...	33
Scheme 4.2	Step of Schiff base complexes formation…….....	36
Scheme 4.3	Proposed hydrolysis of $MSal_2$(di-*t*-Bu)trien in acid solution……..	48
Scheme 4.4	Synthesis of metal-containing polyureas from the reaction between metal complexes and diisocyanates…….	57

LIST OF SYMBOLS AND ABBREVIATION

Sal	Salicylaldehyde
Trien	Triethylenetetramine
$ZnSal_2$trien	bis(salicylaldiminato)triethylenetetramine zinc(II) complex
$ZnSal_2$(OMe)trien	bis(3-methoxysalicylaldiminato)triethylenetetramine zinc(II) complex
$ZnSal_2$(OEt)trien	bis(3-ethoxysalicylaldiminato)triethylenetetramine zinc(II) complex
$ZnSal_2$(di-*t*-Bu)trien	bis(3,5-di-*tert*-butyl-salicylaldiminato)triethylene tetramine zinc(II) complex
$NiSal_2$trien	bis(salicylaldiminato)triethylenetetramine nickel(II) complex
$NiSal_2$(OMe)trien	bis(3-methoxysalicylaldiminato)triethylenetetramine nickel(II) complex
$NiSal_2$(OEt)trien	bis(3-ethoxysalicylaldiminato)triethylenetetramine nickel(II) complex
$NiSal_2$(di-*t*-Bu)trien	bis(3,5-di-*tert*-butyl-salicylaldiminato)triethylene tetramine nickel(II) complex
$Bu_4NCF_3SO_3$	Tetrabutylammonium trifluoromethanesulfonate
Bu_4NOH	Tetrabutylammonium hydroxide
DFT	Density Functional Theory
B3LYP	Becke's Three Parameter Hybrid Functional Using the Lee-Yang-Parr Correlation Functional
K_n^H	Stepwise protonation constant
β	Stability constant
LH_4^{2+}	Schiff base ligand cation
LH_2	Schiff base ligand
L^{2-}	Schiff base ligand anion
ML	Schiff base metal complexes

CHAPTER I

INTRODUCTION

1.1 Schiff base metal complexes

The imine ligands are the products derived from the condensation of carbonyl compounds with primary amines (Scheme 1.1). The obtained ligands are often called Schiff bases.

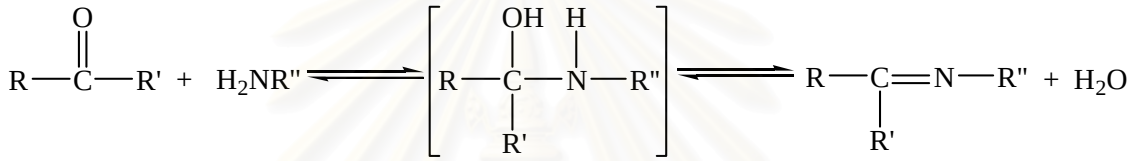

Scheme 1.1 Synthesis of imines.

Schiff base metal complexes have been of interest in coordination chemistry for many years due to their facile synthesis and wide applications [1]. These complexes have significant contribution in the development of catalysis and enzymatic reactions, magnetism, molecular architectures and material chemistry [2-4]. There are numerous examples of the Schiff base complexes derived from salicylaldehydes and hydroxynaphthaldehydes [5]. Examples of the application of these metal complexes are as follows:

Jacobsen and coworkers [6] studied enantioselective epoxidation of simple olefins which is a challenging and important synthetic problem, and chiral salen-based complexes have recently emerged as promising catalysts for these reactions. It was found that the Mn(III) complexes (Figure 1.1) catalyze alkene epoxidation by NaOCl in good yield with high selectivity (Table 1.1).

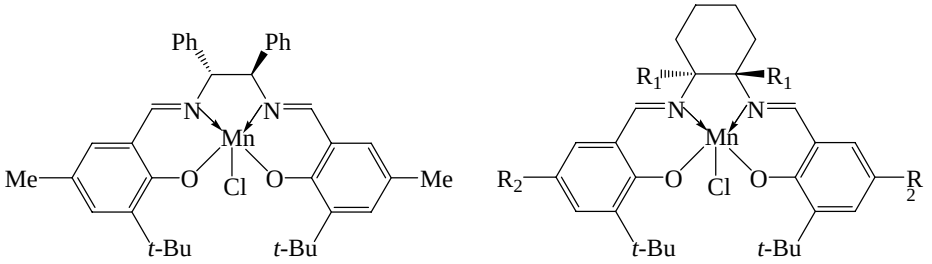

1

2: R_1 = Me, R_2 = Me

3: R_1 = H, R_2 = Me

4: R_1 = Me, R_2 = *t*-Bu

5: R_1 = H, R_2 = *t*-Bu

Figure 1.1 Structure of manganese-salen complexes.

Table 1.1 Asymmetric epoxidation of *cis*-*β*-Methylstyrene with catalysis 1-5.

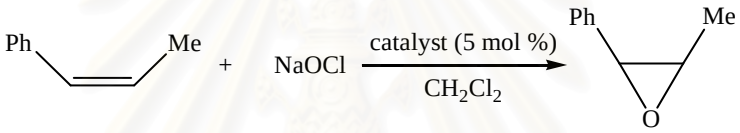

Entry	Catalyst	Yield,[a] %	ee, %	Epoxide configuration
1	(*R*,*R*)-**1**	88	84	1*R*,2*S*-(+)
2	(*S*,*S*)-**2**	54	49	1*S*,2*R*-(-)
3	(*S*,*S*)-**3**	87	80	1*S*,2*R*-(-)
4	(*S*,*S*)-**4**	56	55	1*S*,2*R*-(-)
5	(*S*,*S*)-**5**	81	92	1*S*,2*R*-(-)

[a] Determined by GC by integration against an internal quantitative standard.

Mashhadizadeh and coworkers [7] synthesized a new PVC membrane electrode using *N*-*N*′-bis-(4-dimethylamino-benzylidine)-benzene-1,2-diamine (Figure 1.2) as a suitable neutral carrier. The electrode was used in the direct determination of Ni^{2+} in aqueous solution and as an indicator electrode in potentiometric titration of nickel ion.

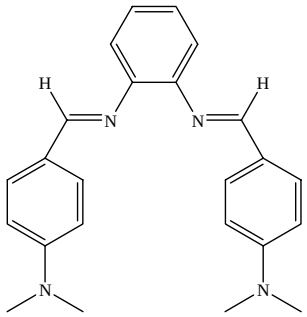

Figure 1.2 Structure of *N-N′*-bis-(4-dimethylamino-benzylidine)-benzene-1,2-diamine

In our previous work, Chantarasiri and coworkers [8] synthesized hexadentate Schiff base metal complexes. The polymerization of diglycidyl ether of bisphenol A (DGEBA) with these metal complexes (Scheme 1.2) gives metal-containing epoxy polymers with good thermal stability. Upon heating at 250 ^{o}C for 48 h, the weight loss of Ni- and Zn-containing epoxy polymer was 2.3 and 3.7%, respectively, which was comparable to that of the epoxy polymer derived from DGEBA/maleic anhydride system.

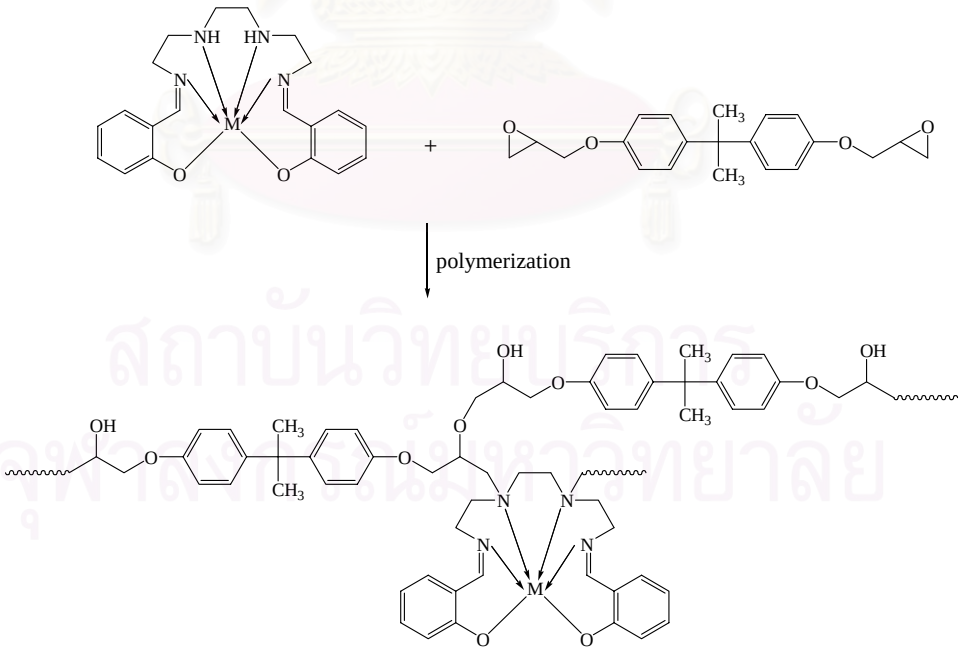

Metal-containing epoxy polymers

M = Ni^{2+} and Zn^{2+}

Scheme 1.2 Synthesis of metal-containing epoxy polymers from DGEBA and hexadentate Schiff base metal complexes.

In 2004, chantarasiri and coworkers [9] also synthesized metal-containing polyureas from polycondensation between metal complexes and diisocyanates (Scheme 1.3). Polymerization of these metal complexes with hexamethylene diisocyanate (HDI) or 4,4′-diphenylmethane diisocyanate (MDI) give metal-containing polyureas in good yields. It was found that the polymers obtained from $ZnSal_2(OMe)trien$ and $NiSal_2(OMe)trien$ are thermally stable.

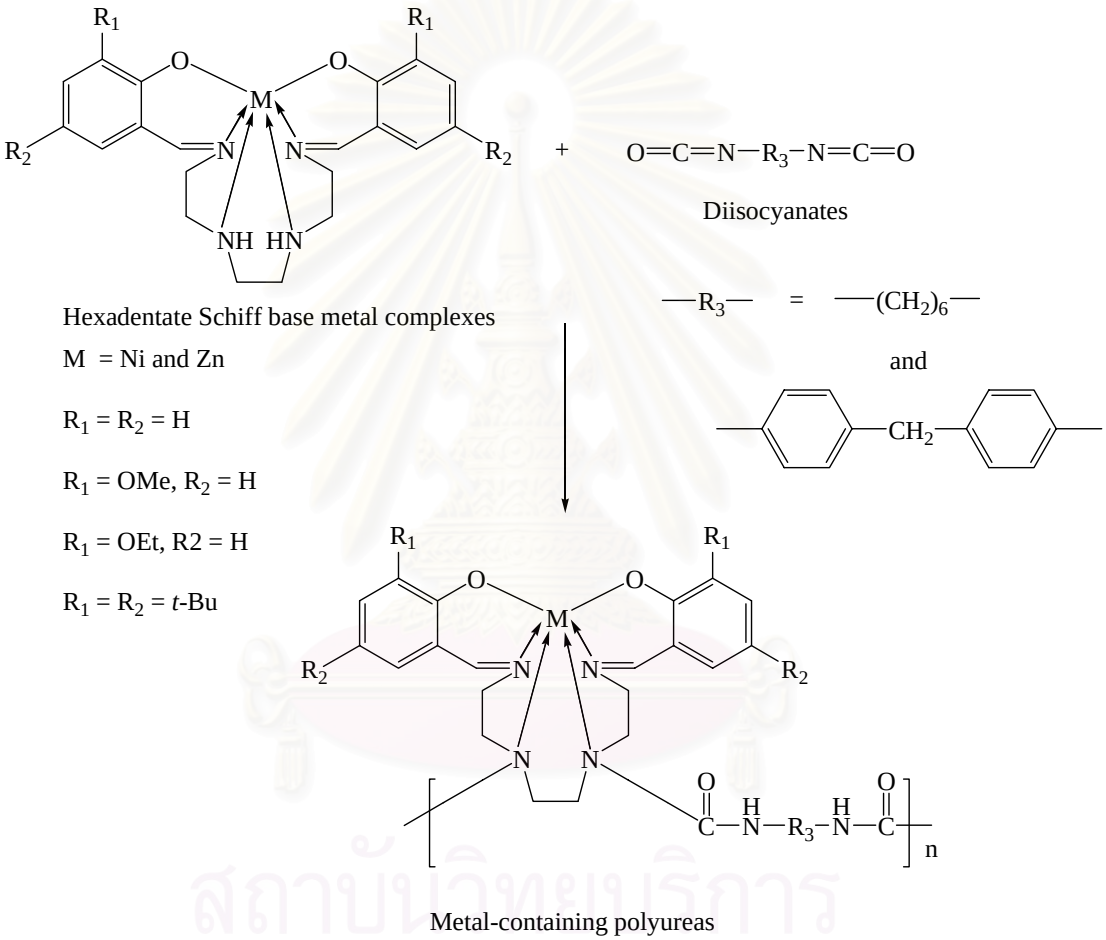

Scheme 1.3 Synthesis of metal-containing polyureas from the reaction between metal complexes and diisocyanates.

1.2 Measurement of protonation constants and stability constants

The main criterion of potentiometric titration is the ligands must be susceptible to protonation. This implies that all ligands, which can be studied by potentiometric method, have to provide proton-acceptable functional group like amines. The

protonation constants may be determined readily using highly accurate pH-electrodes to follow an acid-base titration. Stability constants for the metal complexation reaction are evaluated from an analysis of the various equilibria by a curve fitting computer program such as SUPERQUAD. Examples of such research works are as follows:

Martell and cowokers [10] studied stability of mononuclear and homodinuclear metal complexes with a 24-membered octadentate hexaazamacrocyclic ligand, 3,6,9,17,20,23-hexaaza-29,30-dihydroxy-13,27-dimethyl-tricyclo[23,3,1,1]-1(28),11,13,15(30),25,26-hexaene (BDBPH). A 24-membered hexaazadiphenol macrocyclic ligand was prepared by the $NaBH_4$ reduction of the Schiff base ligand obtained from [2+2] template condensation of 2,6-diformyl-*p*-cresol with diethylenetriamine (Scheme 1.4).

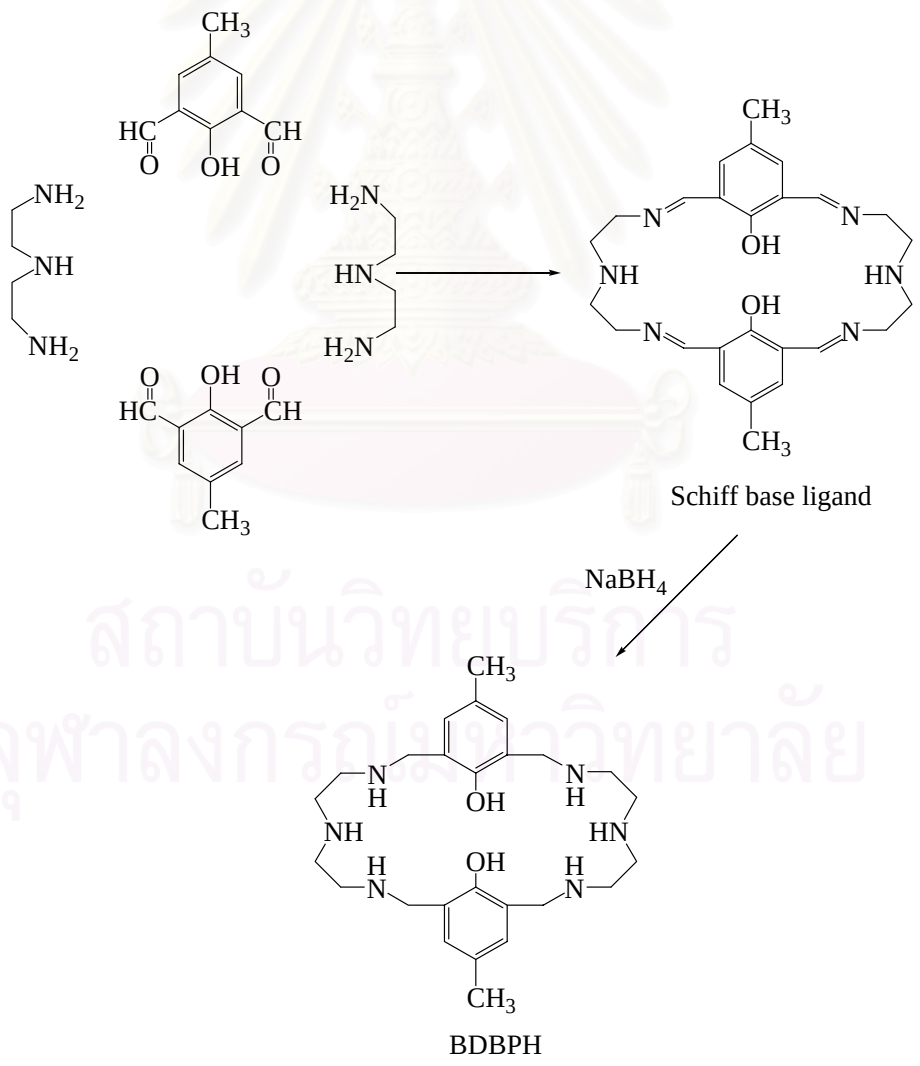

Scheme 1.4 Synthesis of BDBPH.

The stability constants of Ni(II) and Cu(II) with fully deprotonated BDBPH are shown in Table 1.2.

Table 1.2 Log *K* values for the stability constants of the mononuclear and homodinuclear complexes of BDBPH (μ = 0.10 M (KCl), 25 ^{o}C, under argon).

Stepwise quotient K	Log K[a] of BDBPH	
	Ni	Cu
[ML]/[M][L]	12.27	24.50
[MHL]/[ML][H]	10.93	11.08
$[MH_2L]/[MHL][H]$	9.34	9.97
$[MH_3L]/[MH_2L][H]$	5.28	6.30
$[MH_4L]/[MH_3L][H]$	4.23	2.42
$[M_2L]/[ML][M]$[b]	10.85	21.36
$[M_2HL]/[M_2L][H]$	4.04	4.22
$[M_2H_2L]/[M_2HL][H]$	14.87	[c]
$[M_2(OH)L][H]/[M_2L]$	-10.00	[c]
$[M_2(OH)_2L][H]/[M_2(OH)L]$	-11.67	[c]
$[M_2(OH)_3L][H]/[M_2(OH)_2L]$		[c]

[a] Estimated error ± 0.02.

[b] Overall constants is $\log\beta[Ni_2L]/[Ni]^2[L] = 23.12$.

[c] Species not found.

Dechamps-Olivier and coworkers [11] studied the complexation of the unsymmetrical isomers of (2-pyridylmethyl, 3-pyridylmethyl) amine (Figure 1.3) with copper(II) ion.

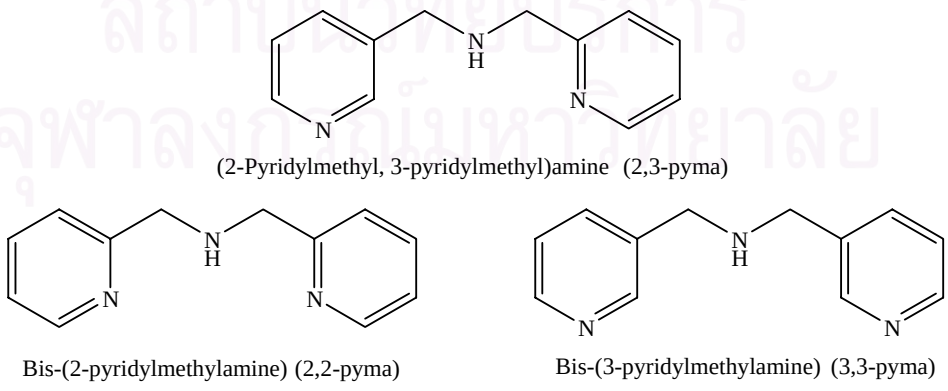

Figure 1.3 Structure of unsymmetrical isomers (2-pyridylmethyl, 3-pyridylmethyl) amine.

The acido-basic behavior of 2,3-pyma in aqueous solution was studied by potentiometric titration. All acidity constants are summarized in Table 1.3. The data for 2,2-pyma and 3,3-pyma are given for comparison. The fully protonated form of the hydrochloride ligand can release three protons: two from the pyridyl groups and one from the amine group. The values of pK_{a1} and pK_{a2} can be attributed to the deprotonation of the two pyridinium groups.

Table 1.3 Acidity constants of unsymmetrical isomers (2-pyridylmethyl, 3-pyridylmethyl) amine.

Ligand	pK_{a1}	pK_{a2}	pK_{a3}
2,3-pyma	1.92 (0.06)	3.85 (0.04)	7.50 (0.02)
2,2-pyma	1.13	2.60	7.28
3,3-pyma	2.95	3.90	7.15

In comparison with the two symmetrical ligands, the first deprotonation (pK_{a1} = 1.92) of 2,3-pyma can be attributed to the 2-substituted pyridyl group and the second deprotonation (pK_{a2} = 3.85) to the 3-substituted pyridyl group. The third deprotonation (pKa3 = 7.50) is then attributed to the secondary amino group. The ligand 2,3-pyma has therefore an acido-basic behavior halfway between 2,2-pyma and 3,3-pyma isomers.

The values obtained for the stability constants (Table 1.4) indicate that the complexes are quite stable. Stability constants obtained for $[CuL]^{2+}$ and $[CuL_2]^{2+}$ complexes in the case of 2,3-pyma ($\log \beta_{110}$ = 8.4 and $\log \beta_{120}$ = 13.8) are lower than those found with 2,2-pyma ($\log \beta_{110}$ = 14.4 and $\log \beta_{120}$ = 19.0). These results can easily be explained by the different coordinating behavior between the two isomers. The ligand 2,2-pyma is known to have a tridentate behavior, while 2,3-pyma has only two nitrogen atoms per ligand that can be linked. The metal ion can only be bonded to the 2-pyridine and the amino group nitrogen atoms simultaneously.

Table 1.4 Stability constants of copper(II) complexes.

Ligand	$\log\beta_{111}$ $[CuLH]^{3+}$	$\log\beta_{110}$ $[CuL]^{2+}$	$\log\beta_{120}$ $[CuL_2]^{2+}$	$\log\beta_{12\text{-}1}$ $[CuL_2(OH)]^{+}$	$\log\beta_{12\text{-}2}$ $[CuL_2(OH)_2]$
2,3-pyma	12.6 (0.1)	8.4 (0.2)	13.8 (0.2)	4.0 (0.1)	-7.5 (0.1)
2,2-pyma	-	14.4	19.0	-	-
3,3-pyma	-	-	-	-	-

1.3 Quantum chemical calculation

Quantum chemical calculation can be give valuable information such as thermodynamic energies of molecules, geometry of molecules, electron density of each atom, etc. For example, a calculation that is described as “6-31G*/STO-3G” indicated that the geometry was determined using the STO-3G basis set and the wave-function was obtained using the 6-31G* basis set. The time-consuming for calculation is depended on efficiency of computer and level of theory for computation.

An example of this research is the work of Lahiri and coworkers [12], which studied crystral structure and geometry-optimization of 2-benzyliminomethylene-4-nitrophenolate. Geometry-optimizations on the monomeric zwitterion (1) and the isomeric hypothetical 2-benzyliminomethylene-4-nitrophenolate (2) molecule by the B3LYP/6-31++G(d,p) method imply an endothermic process [$\Delta H = 12.4$ kcalmol^{-1}] for the transfer of the phenolic proton in the hypothetical neutral molecule to furnish the zwitterionic molecule. As the energy of the neutral molecule is -875.8307 Hartrees and that of the zwitterion is -875.9504 Hartrees, the difference of -12 kcalmol^{-1} shows that the zwitterion structure is more stable of the two structures. Geometry-optimized structures for monomeric zwitterion and 2-benzyliminomethylene-4-nitrophenol are shown in Figure 1.4.

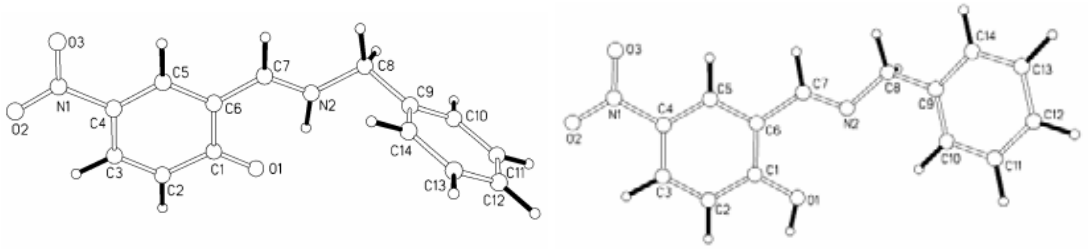

(1) (2)

Figure 1.4 Geometry-optimized structure for monomeric zwitterion and 2-benzyliminomethylene-4-nitrophenol.

Since hexadentate Schiff base metal complexes have useful application in the synthesis of thermally stable polymers, a detailed study in the structure and physico-chemical properties of these metal complexes was carried out to understand the nature of these complexes.

In the course of this study, hexadentate Schiff base zinc and nickel complexes were synthesized. Protonation constants of the hexadentate Schiff base ligands and stability constants of their zinc and nickel complexes were determined by potentiometric titration. The structural energies of the ligands and their complexes were computed using quantum chemical calculations. The result obtained from this work will give the valuable information of the metal complexes such as stability of the complexes and the site of metal complexes that undergoes polymerization reaction. This information can be use in the design of the metal complex structures for future applications.

1.4 Objectives and Scope of this thesis

The main goal of this research is to refine the protonation constants and stability constants for Schiff base ligands and Schiff base metal complexes, respectively. Schiff base metal complexes were synthesized by condensation reaction between salicylaldehyde derivatives, triethylenetetramine and metal acetate (Scheme 1.5).

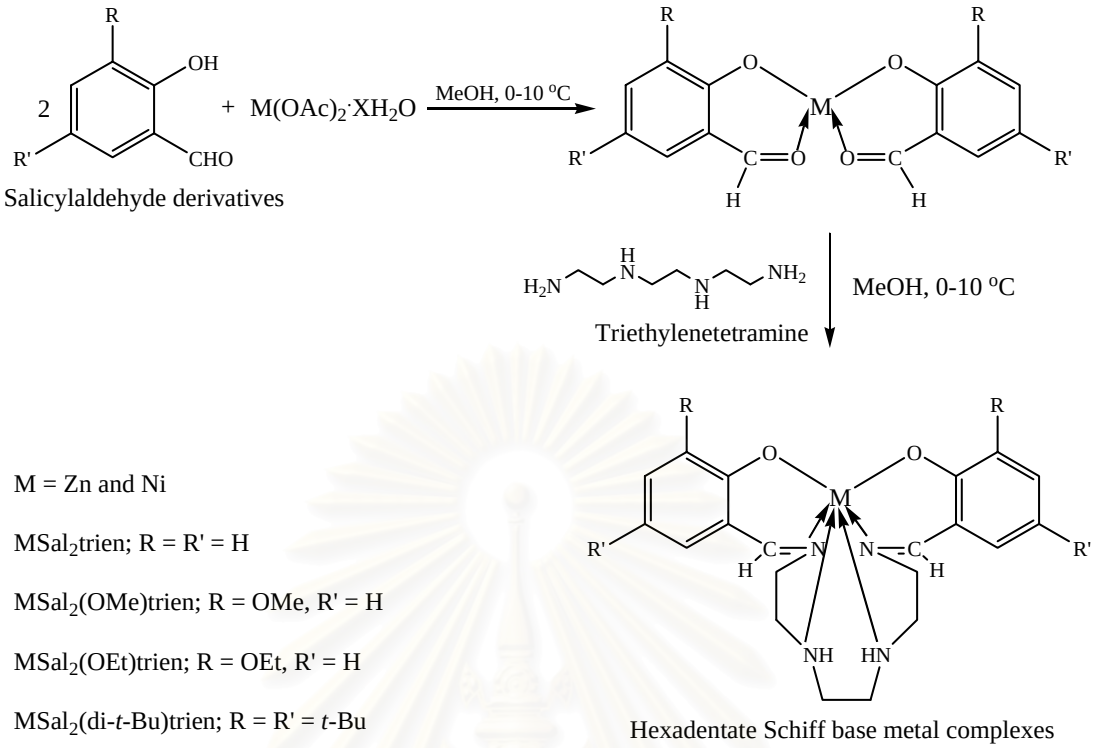

Scheme 1.5 Synthesis of hexadentate Schiff base metal complexes.

Protonation constants and stability constants of Schiff base ligands and Schiff base metal complexes, respectively, were determined by means of potentiometric titrations. Protonation constants and stability constants are evaluated from an analysis of various equilibria by a curve fitting computer program (SUPERQUAD) [13]. Finally, the structures of Schiff base ligands and Schiff base metal complexes were optimized by Density Functional Theory (DFT) calculation using 6-31G basis set. The structural energies of Schiff base ligands and their Schiff base zinc complexes were computed at B3LYP/6-31G(d) level. All structure optimizations and energy calculations were performed with the GAUSSIAN 03 program [14] and graphically interfaced and facilitated by the MOLDEN 3.7 program [15].

CHAPTER II

THEORY

2.1 Chemical equilibrium and potentiometry

2.1.1 Concentration constants and activity constants

An equilibrium constant is quotient involving the concentrations or activities of reacting species in solution at equilibrium. Generally it is defined as ratio of the product of the activities *a* of the reaction products, raised to appropriate power, to the products of the activities of reactants, raised to appropriate power, illustrated by equation (2.1) where a, b, c and d are the stoichiometric coefficients of the solution species A, B, C and D respectively.

$$aA + bB \rightleftharpoons cC + dD \qquad K_{eq} = \frac{a_C^c a_D^d}{a_A^a a_B^b} \tag{2.1}$$

The determination of activities of complex ionic species at both infinite solution and in real solution is a complicated and time-consuming task. However concentrations are related to activities by the expression

$$a_x = [X]\gamma_x \tag{2.2}$$

Where a_x, [X] and γ_x are activity, concentration and activity coefficient of X respectively. Activity coefficients of reacting species are in general tedious and difficult to measure. They also depend very significantly on the nature and concentrations of other species present in solution so that it is not possible to build universal tables of activity coefficients. Theoretical attempts at calculating activity coefficients, based on the Debye-Huckel approach and its extensions, are at the best of only limited accuracy. Substituting the activities from equation (2.2) in (2.1), then the equilibrium constant can be rewritten as follow:

$$K_{eq} = \frac{a_C^c a_D^d}{a_A^a a_B^b} = \frac{[C]^c[D]^d}{[A]^a[B]^b} \cdot \frac{\gamma_C^c \gamma_D^d}{\gamma_A^a \gamma_B^b} \tag{2.3}$$

where [] indicates molar concentrations. If now it is possible to ensure that the term $\frac{\gamma_C^c \gamma_D^d}{\gamma_A^a \gamma_B^b}$ remains constant then the term $\frac{\gamma_A^a \gamma_B^b}{\gamma_C^c \gamma_D^d} . K_{eq}$ is also a constant. Therefore, the equilibrium constant expressed in term of the reacting species, called equilibrium concentration constant, K_c can be written as indicated by equation (2.4).

$$aA + bB \rightleftharpoons cC + dD \qquad K_c = \frac{[C]^c[D]^d}{[A]^a[B]^b} \qquad (2.4)$$

Equilibrium concentration constant, K_c is also known as the stoichiometric equilibrium constant which determined at constant ionic strength where as K_{eq} is indicated by equation (2.1) which is known as an equilibrium activity constant or thermodynamic equilibrium constant.

The term $\frac{\gamma_C^c \gamma_D^d}{\gamma_A^a \gamma_B^b}$ in equation (2.3) may be effectively constant by having a large excess of an inert background electrolyte present and using only low concentrations of reacting ionic species so that any change in their concentrations as a result of their reaction together has an insignificant change on the overall ionic strength of the medium. It is generally possible to replace about 5% of the ions in the inert background electrolyte without appreciably altering the activity coefficients of the minor species present. However, in recording a stoichiometric equilibrium constant it is essential to record not only the concentration of the inert background electrolyte, but also its nature, since the activity coefficient depend on the electrolyte. Consequently, of course, in comparing stoichiometric equilibrium constants, only data obtained under very conditions be used unless the differences between the equilibrium constants are large.

2.1.2 Protonation Constants

The acid-base equilibria of the ligands can be treated by protonation and disprotonation constant. Protonation constant is the equilibrium constant for the addition the n^{th} proton to a charged or uncharged ligand. Protonation constant is knows as basicity constant. The reciprocal of protonation constant is called disprotonation constant and defined as the equilibrium constant for the splitting off n^{th} proton from a

charged or uncharged ligand. Disprotonation constant is also knows as acidity constant. The following equations define these constants and show their interrelation.

$$L + H \rightleftharpoons LH \; ; \; K_1 = \frac{[LH]}{[L][H]} \quad (2.5)$$

$$LH + H \rightleftharpoons LH_2 \; ; \; K_2 = \frac{[LH_2]}{[LH][H]} \quad (2.6)$$

$$LH_2 + H \rightleftharpoons LH_3 \; ; \; K_3 = \frac{[LH_3]}{[LH_2][H]} \quad (2.7)$$

$$\vdots \qquad\qquad \vdots$$

$$LH_{n-1} + H \rightleftharpoons LH_n \; ; \; K_n = \frac{[LH_n]}{[L_{n-1}][H]} \quad (2.8)$$

Another way of expressing the equilibria relations can be show as follow:

$$L + H \rightleftharpoons LH \; ; \; \beta_1 = \frac{[LH]}{[L][H]} \quad (2.9)$$

$$L + 2H \rightleftharpoons LH_2 \; ; \; \beta_2 = \frac{[LH_2]}{[L][H]^2} \quad (2.10)$$

$$L + 3H \rightleftharpoons LH_3 \; ; \; \beta_3 = \frac{[LH_3]}{[L][H]^3} \quad (2.11)$$

$$\vdots \qquad\qquad \vdots$$

$$L + nH \rightleftharpoons LH_n \; ; \; \beta_n = \frac{[LH_n]}{[L][H]^n} \quad (2.12)$$

The K_n's are called the stepwise protonation constants and the β_n's are called the overall or cumulative protonation constants.

2.1.3 Stability Constants

The thermodynamic stability of complex equilibria can be characterized by stability and instability constant. Stability constant is a *n* equilibrium constant for the interaction of metal with ligand. Some time stability is called as formulation constant. In older literature, the inverse of stability constant is used and this is known as instability constant.

If the solution containing metal ions (M) and ligand (L) the system at equilibrium may be described by the following equation and stepwise equilibrium constants.

$$M + L \rightleftharpoons ML \quad ; K_1 = \frac{[ML]}{[M][L]} \tag{2.13}$$

$$ML + L \rightleftharpoons ML_2 \quad ; K_2 = \frac{[ML_2]}{[ML][L]} \tag{2.14}$$

$$ML_2 + L \rightleftharpoons ML_3 \quad ; K_3 = \frac{[ML_3]}{[ML_2][L]} \tag{2.15}$$

$$\vdots \qquad\qquad \vdots$$

$$ML_{n-1} + L \rightleftharpoons ML_n \quad ; K_n = \frac{[ML_n]}{[ML_{n-1}][L]} \tag{2.16}$$

Their will be n such equilibria, where n represents the maximum coordination number of the metal ion M for the ligand L. The cumulative equilibrium constants can be described as followed:

$$M + L \rightleftharpoons ML \quad ; \beta_1 = \frac{[ML]}{[M][L]} \tag{2.17}$$

$$M + 2L \rightleftharpoons ML_2 \quad ; \beta_2 = \frac{[ML_2]}{[M][L]^2} \tag{2.18}$$

$$M + 3L \rightleftharpoons ML_3 \quad ; \beta_3 = \frac{[ML_3]}{[M][L]^3} \tag{2.19}$$

$$\vdots \qquad\qquad \vdots$$

$$M + nL \rightleftharpoons ML_n \quad ; \beta_n = \frac{[ML_n]}{[ML][L]^n} \tag{2.20}$$

Since their can be only independent equilibria in such a system, it is clear that the K_i's and β_i's must be related. The relationship is indeed rather obvious. Consider, for example, the express for β_3 let us multiply both numerator and denominator by $[ML][ML_2]$ and then rearrange slightly:

$$\beta_3 = \frac{[ML_3]}{[M][L]^3} \cdot \frac{[ML][ML_2]}{[ML][ML_2]} \tag{2.21}$$

$$= \frac{[ML]}{[M][L]} \cdot \frac{[ML_2]}{[ML][L]} \cdot \frac{[ML_3]}{[ML_2][L]} \tag{2.22}$$

$$= K_1 \text{ x } K_2 \text{ x } K_3 \tag{2.23}$$

It is not difficult to see that this kind of relationship is perfectly general, namely.

$$\beta_\kappa = K_1 \text{ x } K_2 \text{ x } ... \text{ x } K_k = \prod_{i=1}^{i=k} K_i \qquad (2.24)$$

2.1.4 Secondary concentration variables

In order to evaluate the stability constant (*K*) for a simple system, in theory, it is necessary to prepare a single solution containing a know total amount of metal ion $[M]_T$ and ligand $[L]_T$ and measure one of the three remaining unknown concentrations. These are the free metal ion concentration [M], the free ligand concentration [L] and the metal-ligand complex concentration [ML].

In order evaluate these stability constants, it is necessary to find a relationship between them and the experimentally determined variables ([M], [L], [H] etc). This relationship is often established via the definition of secondary concentration variables. It is from these variables that the stability constants are calculated.

2.1.4.1 The protonation formationfunction $(\bar{P})$

Protonation equilibria of a ligand **L** interacting in a solution of constant ionic strength can be written as follow:

$$L + H \rightleftharpoons LH : K_1 = \frac{[LH]}{[L][H]} \qquad (2.25)$$

$$LH + H \rightleftharpoons LH_2 : K_2 = \frac{[LH_2]}{[LH][H]} \qquad (2.26)$$

$$\vdots \qquad \vdots \qquad \vdots$$

$$LH_{n-1} + H \rightleftharpoons LH_n : K_n = \frac{[LH_n]}{[LH_{n-1}][H]} \qquad (2.27)$$

When n is a number of the proton bind to the ligand **L**. The mass balance equatons for the total concentration of the ligand and proton can be written below.

$$[L]_T = [L] + [LH] + [LH_2] + \ldots + [LH_n] \qquad (2.28)$$

$$[H]_T = [H] + [LH] + 2[LH_2] + \ldots + n[LH_n] \qquad (2.29)$$

A function $\bar{p}$ defined as the average number of proton **H** bring to the ligand **L**:

$$\bar{P} = \frac{\text{total bond proton}}{\text{total ligand}} = \frac{[H^+]_T - [H^+] + [OH^-]}{[L]_T} \quad (2.30)$$

When $[H^+]$ is concentration of the free proton obtained from the measurement. $[OH^-]$ is the concentration due to the titrant which can be converted to $[H^+]$ via the relation of the autoprotolysis constant of methanol.

2.1.4.2 The complex formation function $(\bar{n})$

Let us consider a metal ion **M** and a ligand **L** interacting in solution of constant ionic strength. The equilibria present are:

$$M + L \rightleftharpoons ML : K_1 = \frac{[ML]}{[M][L]} \quad (2.31)$$

$$ML + L \rightleftharpoons ML_2 : K_2 = \frac{[ML_2]}{[ML][L]} \quad (2.32)$$

$$\vdots \qquad \vdots \qquad \vdots$$

$$ML_{n-1} + L \rightleftharpoons ML_n : K_n = \frac{[ML_n]}{[ML_{n-1}][L]} \quad (2.33)$$

The maximum value of n, written N, will be a function of both the maximum coordination number of the metal ion and the multidentate nature of the ligand. We can now write mass balance equations for both the total metal ion and total ligand concentrations.

$$[M]_T = [M] + [ML] + [ML_2] + \ldots + [ML_n] \quad (2.34)$$

$$[L]_T = [L] + [ML] + 2[ML_2] + \ldots + n[ML_n] \quad (2.35)$$

A function $\bar{n}$ defined as the average number of ligands **L** attached to the metal **M** may be written

$$\bar{n} = \frac{\text{total bond ligand}}{\text{total metal}} = \frac{[L]_T - [L]}{[M]_T} \quad (2.36)$$

Substituting equation (2.34) and (2.35) in (2.36) yields

$$\bar{n} = \frac{[ML] + 2[ML_2] + ... + n[ML_n]}{[M]+[ML]+[ML_2]+...+ [ML_n]} \quad (2.37)$$

In summation term equation (2.37) becomes

$$\bar{n} = \frac{\sum_{n=1}^{n=N} n[ML_n]}{[M] + \sum_{n=1}^{n=N} n[ML_n]} \quad (2.38)$$

where N is the maximum coordination number for the metal if L is a monodentate ligand. However K_n and β_n are defined by

$$K_n = \frac{[ML_n]}{[ML_{n-1}][L]} \quad (2.39)$$

$$\beta_n = \frac{[ML_n]}{[M][L]^n} \quad (2.40)$$

In addition, $$\beta n = K_1K_2K_3 \ldots K_n \quad (2.41)$$

and on substituting equation (2.39) into (2.37) gives

$$\bar{n} = \frac{K_1[M][L] + 2K_1K_2[M][L]^2 + ... + nK_1K_2 ... K_n[ML]}{[M] + K_1[M][L] + K_1K_2[M][L]^2 + ... + K_1K_2 ... K_n[M][L]^n} \quad (2.42)$$

and after dividing through by [M] and remembering equation (2.41)

$$\bar{n} = \frac{\beta_1[L] + 2\beta_2[L]^2 + ... + n\beta_n[L]^n}{1 + \beta_1[L] + \beta[L]^2 + ... + \beta_n[L]^n} \quad (2.43)$$

which may be more conveniently written in summation terms

$$\bar{n} = \frac{\sum_{n=1}^{n=N} n\beta_n[L]^n}{1 + \sum_{n=1}^{n=N} \beta_n[L]^n} \equiv \frac{\sum_{n=1}^{n=N} n\beta_n[L]^n}{\sum_{n=0}^{n=N} \beta_n[L]^n} \quad (2.44)$$

It is immediately apparent from equation (2.44). That n is solely dependent on the free ligand concentration, [L], and is independent of $[M]_T$, $[L]_T$ and the free metal ion concentration [M]. The complex formation function, $\bar{n}$, is the starting point for many of the methods used in the calculation of stability constants.

2.1.5 Computation of equilibrium constants by SUPERQUAD program

The computer program, SUPERQUAD has been widely used to calculate stability constants species in solution equilibria from data obtained by potentiometric method. The formation constants are determined by minimization of an error-square sum based on measure electrode potentials. The program also permits refinement of any reactant concentration or standard electrode potential. The refinement is incorporated in to new procedure which can be used for model selection. The assumptions for formation constants by SUPERQUAD could be described as follows.

Assumptions: There are number of assumptions underlying the whole treatment, and each needs to be considered explicitly.

1. For each chemical species $A_aB_b\ldots$ in the solution equilibria, there is a chemical constant, the formation constant, which is expressed as a concentration quotient in equation (2.45)

$$\beta_{ab\ldots} = \frac{[AaBb...]}{[A]^a[B]^b...} \qquad (2.45)$$

A, B… are the reactants (SUPEQUAD allows up to four of term) and [A], [B] are the concentrations of free reactant; electrical charges may be attached to any species, but there are omitted for sake of simplicity in this discussion. Since the thermodynamic definition of a formation constant is as an activity quotient, it is to be assumed that the quotient of the activity coefficients is constant, an assumption usually justified by performing the experiments with a medium of high ionic strength.

2. Each electrode present exhibits a pseudo-Nernstain behavior, equation (2.46), where [A] is the concentration of the electro-active ion,

$$E = E^{o} + S_L \log[A] \qquad (2.46)$$

E is the measured potential, and E^{o} is the standard electrode potential. The ideal value of the slope S_L is of course *RT/nF*, but we assume only that it is a constant for a given electrode. The value of E^{o} and S_L are usually obtained in separate calibration experiment. Further there is a modified Nernst equation.

$$E = E^{o} + S_L \log[H^{+}] + r[H^{+}] + s[H^{+}]^{-1} \qquad (2.47)$$

This equation was first suggested as means of taking into account junction potentials in strongly acidic and strongly basic condition.

3. Systematic errors must be minimized by careful experimental work. Sources of systematic error include electrode calibration, sample weighing and dilutions, standardization of reagents (use of carbonate-free alkali in particular), temperature variation and water quality. The last-named factor is more significant today than it was in the past, as water may be contaminated by titrable species which can pass through distillation columns by surface action. All statistical tests are based on the assumption that systematic errors are absent from the data.

4. The independent variable is not subject to error. Errors in the dependent variable are assumed to have a normal distribution. If these assumptions are true use of the principle of least squares will yield a maximum likelihood result, and computed residuals should not show systematic trends.

5. There exits a model of the equilibrium system, which adequately accounts for the experimental observations. The model is specified by a set of coefficients a, b,…, one for each species formed. All least-squares refinements are performed in term of an assumed model. Examination of sequence of models should yield a best model which is not significantly different from the true model. Choice of the best model is know as species selection.

2.2 Quantum chemical calculation

2.2.1 Basis set effects

A basis set is the mathematical description of the orbitals with in a system which in turn combine to approximate the total electronic wave-function, used to perform the theoretical calculation. Larger basis set more accurately approximate the orbitals by imposing fewer restrictions on the locations of the electrons in space. In the true quantum mechanical picture, electrons have affinity probability of existing anywhere in space; this limit corresponds to the infinite basis set expansion.

Standard basis set for electronic structure calculations use linear combinations of GAUSSIAN functions to form the orbitals. GAUSSIAN program offers a wide range of predefined basis set, which may be classified by the number and types of basis functions that they contain. Basis sets assign a group of basis functions to each atom within a molecule to approximate is orbitals. These basis function themselves are composed of a linear of GAUSSIAN function; such basis functions are referred to as contracted functions, and the component GAUSSIAN functions are referred to as primitives. A basis function consisting of a single GAUSSIAN function is termed uncontracted.

2.2.1.1 Minimal basis sets

Minimal basis sets contain the minimum number of functions needed for each atom, as in these examples:

H: 1s

C: 1s, 2s, $2p_x$, $2p_y$, $2p_z$

Minimal basis sets use fixed-size atomic-type orbitals. The STO-3G basis set [16] is a minimal basis set (although it is not the smallest possible basis set). It uses three GAUSSIAN primitives per basis function, which accounts for the “3G” in its name. “STO” stands for “Slater-type orbitals” and the STO-3G basis set approximates Slater orbitals with GAUSSIAN functions.

2.2.1.2 Split valence basis sets

The first way that a basis set can be made larger is to increase the number of basis functions per atom. Split valence basis sets, such as 6-31G [17-21], have two or more sizes of basis function for each valence orbital. For example, hydrogen and carbon are represented as:

H: 1s, 1s′

C: 1s, 2s, 2s′, $2p_x$, $2p_x'$, $2p_y$, $2p_y'$, $2p_z$, $2p_z'$

where the primed and unprimed orbitals differ in size.

The double zeta basis sets, such as the Dunning-Huzinage basis set (D95) [22], form all molecular orbitals from linear combinations of two sizes of functions for each atomic orbital. Similarly, triple split valence basis sets, like 6-311G [23-29], use three sizes of contracted functions for orbital-type.

2.2.1.3 Practical considerations when performing *ab initio* calculations

Ab inintio calculations can be extremely time-consuming, especially when using the high levels of theory or when the nuclei are free to move, as in a minimization calculation. Various “tricks” have been developed which can significantly reduced the computational effort involved. Many of these options are routinely available in the major software packages and are invoked by the specification of simple keywords. One common tactic is to combine different levels of theory for the various stages of a calculation. For example, a lower level of theory can be used provide the initial guess for the density matrix prior to the first SCF iteration. Lower levels of theory can also be used in other ways. Suppose we wish to determine some of the electron properties of a molecule in a minimum energy structure. Energy minimization requires that the nuclei move, and is typically performed in a series of steps, at each of which the energy (and frequently the gradient of the energy) must be calculated. Minimization is therefore a computationally expensive procedure, particularly when performed at the high level of theory. To reduce this computational burden a lower level of theory can be employed for the geometry optimization. A “single point” calculation using a high level of theory is the performed at the geometry so obtained to give a wave-function from which the

properties are determined. The assumption here of course is that the geometry does not change much between the two levels of theory. Such calculations are denoted by slashes (/). For example, a calculation that is described as “6-31G*/STO-3G” indicates that the geometry was determined using the STO-3G basis set and the wave-function was obtained using the 6-31G* basis set. Two slashes are used when each calculation is itself described using a slash, such as when electron correlation methods are used. For example, “MP2/6-31G*//HF/6-31G*” indicates a geometry optimization using a Hartree-Fock calculation with a 6-31G* basis set followed by a single-point calculation using the MP2 method for incorporating electron correlation, again using a 6-31G* basis set.

2.2.1.4 Setting up the calculation and choice of coordinates

The traditional way to provide the nuclear coordinates to a quantum mechanical program is via a Z-matrix, in which the positions of the nuclei are defined in terms of a set of internal coordinates. Some programs also accept coordinates in Cartesien format, which can be more convenient for large system. It can sometime be important to choose an appropriate set of internal coordinates, especially when locating minima or transition points or when following reaction pathways.

2.2.1.5 Calculating derivatives of the energy

Considerable effort has been spent devising efficient ways of calculating the first and second derivatives of the energy with respect to the nuclear coordinates. Derivatives are primarily used during minimization procedures for finding equilibrium structures and are also used by methods, which locate transition structure and determine reaction pathways. To calculate derivatives of the energy it is necessary to calculate the derivatives of the various electron integrals. For GAUSSIAN basis sets the derivatives can be obtained analytically, and it is relatively straightforward to obtain first derivatives for many level of theory. The time taken to calculate the derivatives are comparable to that requires for the calculation of the total energy. Second derivatives are more difficult and expensive to calculate, even at the lower levels of theory.

CHAPTER III

EXPERIMENTAL

3.1 Materials

All reagents and solvents were analytical grade quality. Zinc (II) acetate dihydrate, nickel (II) acetate tetrahydrate, salicylaldehyde, 3-methoxysalicylaldehyde, triethylenetetramine and tetrabutylammonium trifluoromethanesulfonate ($Bu_4NCF_3SO_3$) were obtained from the Fluka. 3-Ethoxysalicylaldehyde and 3,5-di-tert-butyl-2-hydroxybenzaldehyde were obtained from Aldrich. Tetrabutylammonium hydroxide (Bu_4NOH) was obtained from Riedel-de Haen. All chemicals were used without further purification.

3.2 Analytical Procedures

IR spectra were recorded on a Nicolet Impact 410 using KBr pellet method. NMR spectra were recorded in $CDCl_3$ and DMSO-d_6 solution on a Varian Mercury-400 BB instrument. Chemical shifts are given in parts per million (ppm) using the proton residual as internal reference. All potentiometric titrations were performed on an automatic titrator model DL25 (Mettler, Switzerland). The temperature during all titration experiment was controlled at 25 ± 0.1 ^{o}C by external circulation of Heto DT-2 thermostat (Denmark). The concentrations of free proton [H^+] in observed solution were measured by combined pH electrode model DG 113-SC (Mettler, Switzerland) connected to an automatic titrator. All structure optimizations and energy calculations were performed with the GAUSSIAN 03 program and graphically interfaced and facilitated by the MOLDEN 3.7 program.

3.3 Synthetic Procedure

All metal complexes were prepared according to the method reported in the literature [8-9]. The spectroscopic data of all metal complexes are in good agreement with these reported in the literature.

3.3.1 Synthesis of hexadentate Schiff base zinc complexes

3.3.1.1 Preparation of bis(salicylaldiminato)triethylenetetramine zinc(II) complex [$ZnSal_2trien$]

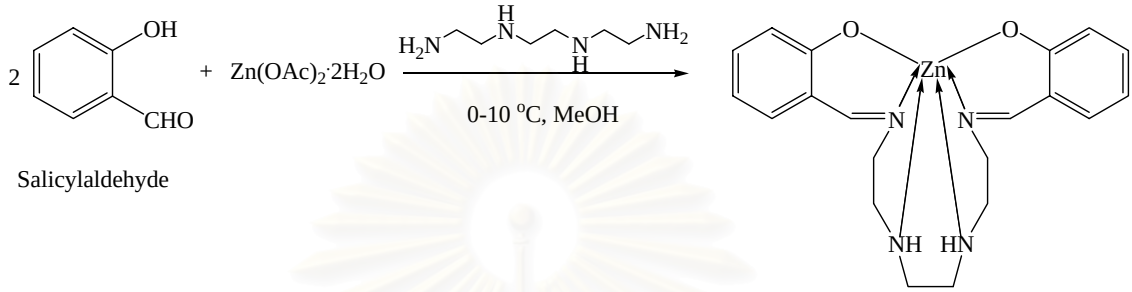

Salicylaldehyde

$ZnSal_2trien$

$ZnSal_2trien$ was prepared according to the method as follows: a solution of salicylaldehyde (0.244 g, 2.0 mmol) and Zn(II) acetatedihydrate (0.220 g, 1.0 mmol) in methanol (15 mL) was prepared at 0 ^oC. To this solution, triethylenetetramine (0.149 mL, 1.0 mmol) in methanol (15 mL) was added dropwise over a period of 20 min. After stirring at 0 ^oC for 15 min, a solution of 2 N sodium hydroxide (1.0 mL, 2.0 mmol) was added and the reaction mixture was stirred at room temperature for 1 h. $ZnSal_2trien$ crystals was obtained as pale yellow crystalline solid by slow evaporation of methanol from the reaction mixture at room temperature. The yellow crystals were filtated and dried in vacuo to yield 0.387 g (93%) of $ZnSal_2trien$.

3.3.1.2 Preparation of bis(3-methoxysalicylaldiminato)triethylenetetramine zinc(II) complex [$ZnSal_2(OMe)trien$]

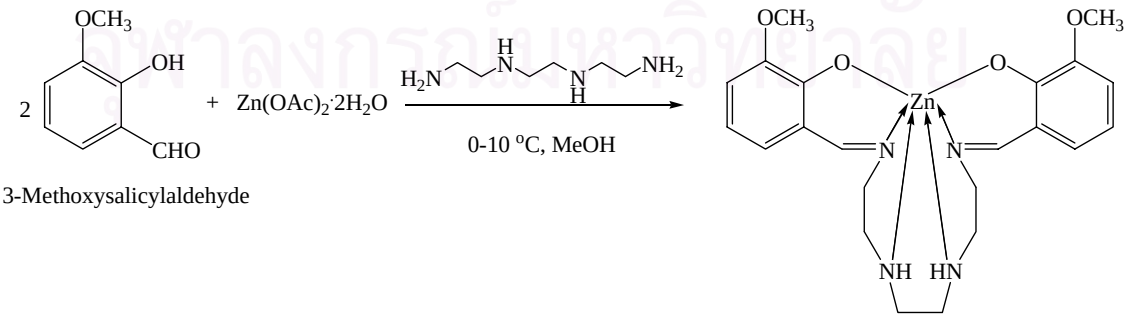

3-Methoxysalicylaldehyde

$ZnSal_2(OMe)trien$

$ZnSal_2$(OMe)trien was synthesized in the same manner as $ZnSal_2$trien using o-vanillin (3-methoxysalicylaldehyde) (0.304 g, 2.0 mmol) instead of salicylaldehyde. $ZnSal_2$(OMe)trien was obtained as yellow crystalline solid (0.289 g, 61%).

3.3.1.3 Preparation of bis(3-ethoxysalicylaldiminato)triethylenetetramine zinc(II) complex [$ZnSal_2$(OEt)trien]

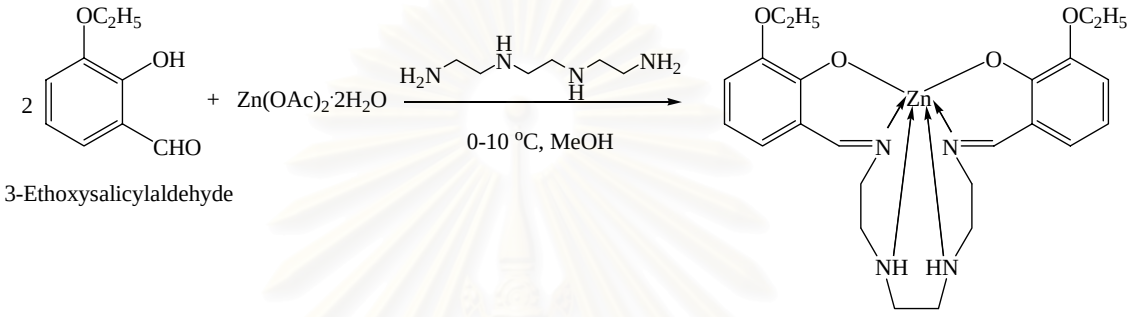

3-Ethoxysalicylaldehyde

$ZnSal_2$(OEt)trien

$ZnSal_2$(OEt)trien was synthesized in the same manner as $ZnSal_2$trien using 3-ethoxysalicylaldehyde (0.332 g, 2.0 mmol) instead of salicylaldehyde. $ZnSal_2$(OEt)trien was obtained as yellow crystalline solid (0.468 g, 93%).

3.3.1.4 Preparation of bis(3,5-di-*tert*-butyl-salicylaldiminato)triethylene tetramine zinc(II) complex [$ZnSal_2$(di-*t*-Bu)trien]

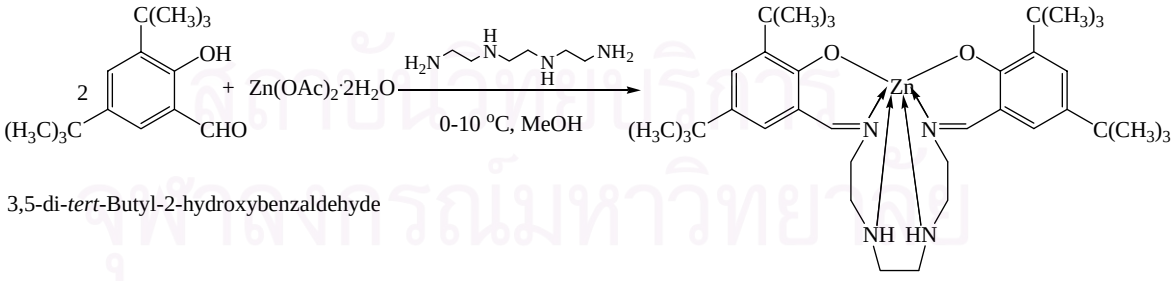

3,5-di-*tert*-Butyl-2-hydroxybenzaldehyde

$ZnSal_2$(di-*t*-Bu)trien

$ZnSal_2$(di-*t*-Bu)trien was synthesized in the same manner as $ZnSal_2$trien using 3,5-di-*tert*-butyl-2-hydroxybenzaldehyde (0.469 g, 2.0 mmol) instead of salicylaldehyde. $ZnSal_2$(di-*t*-Bu)trien was obtained as yellow crystalline solid (0.540 g, 84%).

3.3.2 Synthesis of hexadentate Schiff base nickel complexes

3.3.2.1 Preparation of bis(salicylaldiminato)triethylenetetramine nickel(II) complex [$NiSal_2trien$]

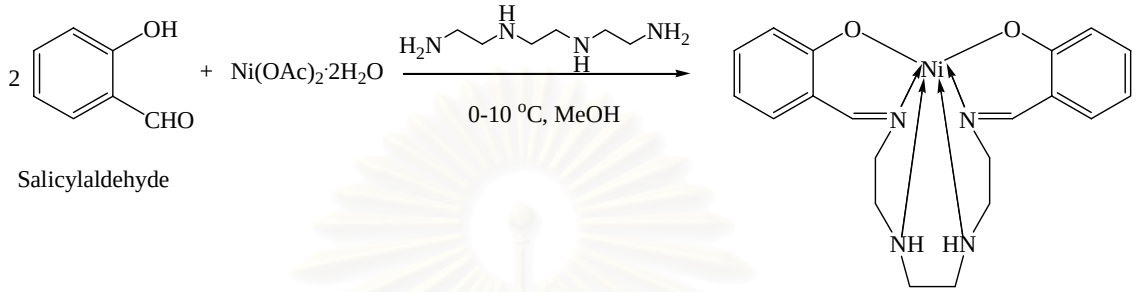

Salicylaldehyde

$NiSal_2trien$

$NiSal_2trien$ was prepared according to the method as follows: a solution of salicylaldehyde (0.244 g, 2.0 mmol) and Ni(II) acetatedihydrate (0.249 g, 1.0 mmol) in methanol (15 mL) was prepared at 0 ^{o}C. To this solution, triethylenetetramine (0.149 mL, 1.0 mmol) in methanol (15 mL) was added dropwise over a period of 20 min. After stirring at 0 ^{o}C for 15 min, a solution of 2 N sodium hydroxide (1.0 mL, 2.0 mmol) was added and the reaction mixture was stirred at room temperature for 1 h. The brown crystal were filtered and dried in vacuo to yield 0.250 g (61%) of $NiSal_2trien$.

3.3.2.2 Preparation of bis(3-methoxysalicylaldiminato)triethylenetetramine nickel(II) complex [$NiSal_2(OMe)trien$]

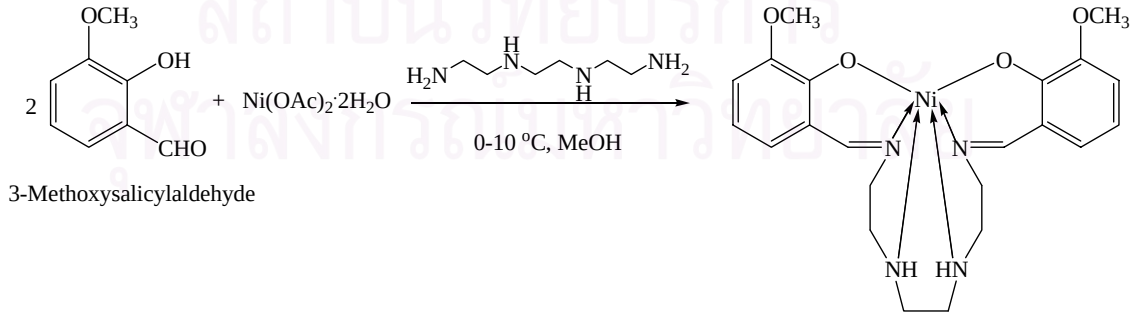

3-Methoxysalicylaldehyde

$NiSal_2(OMe)trien$

$NiSal_2$(OMe)trien was synthesized in the same manner as $NiSal_2$trien using o-vanillin (3-methoxysalicylaldehyde) (0.304 g, 2.0 mmol) instead of salicylaldehyde. $NiSal_2$(OMe)trien was obtained as brown crystalline solid (0.210 g, 45%).

3.3.2.3 Preparation of bis(3-ethoxysalicylaldiminato)triethylenetetramine nickel(II) complex [$NiSal_2$(OEt)trien]

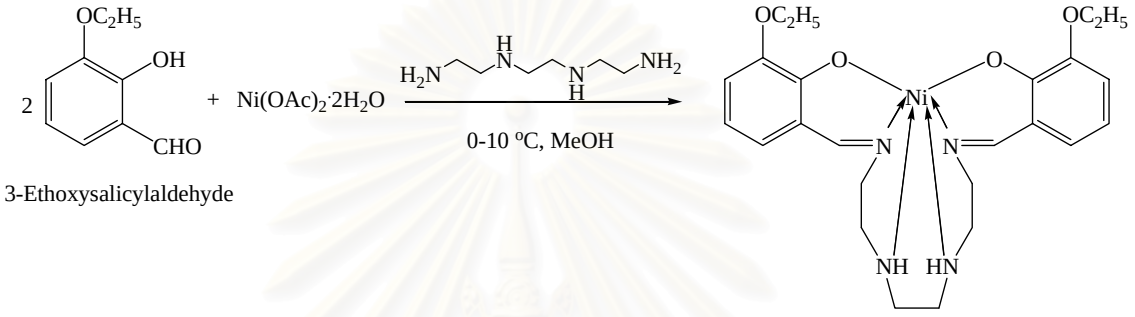

3-Ethoxysalicylaldehyde

$NiSal_2$(OEt)trien

$NiSal_2$(OEt)trien was synthesized in the same manner as $NiSal_2$trien using 3-ethoxysalicylaldehyde (0.332 g, 2.0 mmol) instead of salicylaldehyde. $NiSal_2$(OEt)trien was obtained as brown crystalline solid (0.490 g, 98%).

3.3.2.4 Preparation of bis(3,5-di-*tert*-butyl-salicylaldiminato)triethylene tetramine nickel(II) complex [$NiSal_2$(di-*t*-Bu)trien]

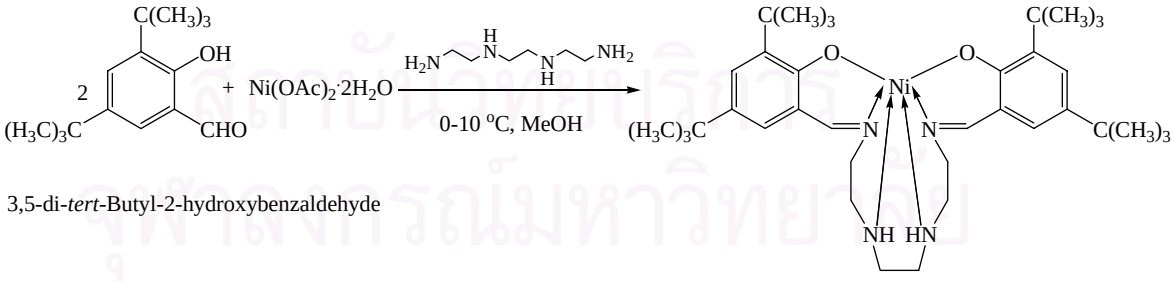

3,5-di-*tert*-Butyl-2-hydroxybenzaldehyde

$NiSal_2$(di-*t*-Bu)trien

$NiSal_2$(di-*t*-Bu)trien was synthesized in the same manner as $NiSal_2$trien using 3,5-di-*tert*-butyl-2-hydroxybenzaldehyde (0.469 g, 2.0 mmol) instead of salicylaldehyde. $NiSal_2$(di-*t*-Bu)trien was obtained as brown crystalline solid (0.451 g, 71%).

3.4 Potentiometric measurements

Protonation constants of ligand, Sal_2trien, Sal_2(OMe)trien and Sal_2(OEt)trien and stability constants of their zinc and nickel complexes, $ZnSal_2$trien, $ZnSal_2$(OMe)trien, $ZnSal_2$(OEt)trien, $NiSal_2$trien, $NiSal_2$(OMe)trien and $NiSal_2$(OEt)trien were determined by means of potentiometric titration. Concentrations of free hydrogen ion [H^+] in the solution were measured by a combined electrode (Mettler DG 113-SC) connected to an automatic titrator (Mettler DL 25) at 25 ^oC. The electrode was calibrated at pH (-log[H^+]) = 2.0 with standard solution of 1.0 x 10^{-2} M $HClO_4$ by adjusting the Nernstian slope based on the isopotential point of pH 8.30 = 0.0 mV. According to the junction potentials of the electrode, the pH of the solution can be corrected by using the following formular [30]

$$pH_{corrected} = pH_{observed} + a + b[H^+]_{observed}$$

The constants *a* and *b* were determined from the pH measurements of the solution of 1.0 x 10^{-3} M $HClO_4$ and 1.00 x 10^{-2} M $Bu_4NCF_3SO_3$ prepared in MeOH and potentiometric titration were carried out at 25 ^oC with deviation of ± 0.1 ^oC, regulated by an external EtOH DT-2 thermostat. The titrations were performed under argon atmosphere. Typically, 10 mL of the complex solution was titrated with the Bu_4NOH solution in a temperature-controlled beaker. The complex concentration was varied from 7.50 x 10^{-4} to 1.10 x 10^{-3} M. At least 40 points of each potentiometric titration were used in computations for the equilibrium constants. The solution of the electrolyte was obtained by dissolution of a weighed quantity of $Bu_4NCF_3SO_3$ in methanol. The ionic strength was kept at 1.0 x 10^{-2} M for all experiments. The solution of zinc and nickel complexes (1.0 x 10^{-3} M) and their corresponding titrant base, Bu_4NOH (5.0 x 10^{-2} M), were prepared in $Bu_4NCF_3SO_3$ (1.0 x 10^{-2} M) in MeOH. A standard solution of $HClO_4$ (1.0 x 10^{-2} M) in the background electrolyte was used to adjust the pH of the working solution. Finally, the solution was titrated with standard Bu_4NOH solution. The experimental data for protonation and complexation with zinc and nickel were shown in Tables 3.1 and 3.2, respectively.

Table 3.1 Experimental data for determining the protonation constants and stability constants of zinc complexes.

Complexes	Titration	Initial concentration (M)		pH range	Number of data points
		Metal complexes	Proton		
$ZnSal_2$trien	1	9.082×10^{-4}	4.379×10^{-3}	2.745-11.456	90
	2	8.325×10^{-4}	8.028×10^{-3}	2.205-10.827	71
	3	7.992×10^{-4}	9.634×10^{-3}	2.043-9.235	59
	4	7.685×10^{-4}	1.112×10^{-2}	1.972-11.228	85
$ZnSal_2$(OMe)trien	1	9.990×10^{-4}	0	9.464-11.482	34
	2	9.082×10^{-4}	4.459×10^{-3}	3.295-11.432	91
	3	8.687×10^{-4}	6.391×10^{-3}	2.734-11.217	88
	4	8.325×10^{-4}	8.167×10^{-3}	2.543-11.005	81
$ZnSal_2$(OEt)trien	1	9.524×10^{-4}	1.946×10^{-3}	4.773-11.277	66
	2	9.091×10^{-4}	3.714×10^{-3}	3.095-11.355	87
	3	8.696×10^{-4}	5.330×10^{-3}	2.655-11.147	80
	4	8.333×10^{-4}	6.810×10^{-3}	2.450-10.790	75
$ZnSal_2$(di-*t*-Bu) trien	1	9.505×10^{-4}	2.664×10^{-3}	5.156-11.156	61
	2	9.073×10^{-4}	3.377×10^{-3}	3.173-11.253	82
	3	8.678×10^{-4}	4.096×10^{-3}	2.741-10.980	76
	4	8.317×10^{-4}	5.477×10^{-3}	2.461-8.971	57

Table 3.2 Experimental data for determining the protonation constants and stability constants of nickel complexes.

Complexes	Titration	Initial concentration (M)		pH range	Number of data points
		Metal complexes	Proton		
$NiSal_2$trien	1	9.505×10^{-4}	2.464×10^{-3}	2.678-11.447	79
	2	9.073×10^{-4}	4.703×10^{-3}	2.203-11.039	69
	3	8.317×10^{-4}	8.622×10^{-3}	1.875-10.173	57
	4	7.984×10^{-4}	1.035×10^{-2}	1.825-10.931	59
$NiSal_2$(OMe)trien	1	9.505×10^{-4}	2.004×10^{-3}	3.120-11.446	80
	2	9.073×10^{-4}	3.825×10^{-3}	2.591-11.232	75
	3	8.678×10^{-4}	5.489×10^{-3}	2.503-11.378	72
	4	8.317×10^{-4}	7.013×10^{-3}	2.375-11.139	73
$NiSal_2$(OEt)trien	1	9.524×10^{-4}	2.226×10^{-3}	2.779-11.403	72
	2	9.091×10^{-4}	4.248×10^{-3}	2.242-11.105	75
	3	8.696×10^{-4}	6.096×10^{-3}	2.143-11.269	67
	4	8.333×10^{-4}	7.788×10^{-3}	2.059-11.371	73
$NiSal_2$(di-*t*-Bu) trien	1	9.514×10^{-4}	2.004×10^{-3}	2.874-11.470	50
	2	9.082×10^{-4}	3.825×10^{-3}	2.482-11.201	55
	3	8.325×10^{-4}	7.013×10^{-3}	2.340-10.957	60
	4	7.992×10^{-4}	8.416×10^{-3}	2.227-11.092	71

The experimental data were evaluated by the computer program SUPERQUAD. The results were reported in term of the logarithm of overall equilibrium constants. For determination of stability constants of complexation, these formation constants were calculated together with protonation constants.

3.5 Quantum chemical calculations

The calculations were carried out using the GAUSSIAN 03 package of programs. The computational method is Becke's gradient-corrected exchange-correlation density functionals (B3LYP) [31-32]. According to the theorem of Hohenberg and Kohn [33], the functionals employed by DFT methods partition the electronic energy *E* of a molecule into the terms

$$E(\rho) = E^{T}(\rho) + E^{V}(\rho) + E^{J}(\rho) + E^{XC}(\rho)$$

where E^{T} is the kinetic energy of the electrons, E^{V} is the potential energy of nuclear-electron attraction and nuclear-nuclear repulsion, E^{J} is the electron-electron repulsion of the classical energy of density ρ, and E^{XC} is the exchange (X) arising from the wave function including the dynamical correlation (C) of electron motion. The term E^{XC} is divided into two separate functionals

$$E^{XC}(\rho) = E^{X}(\rho) + E^{C}(\rho)$$

The definition of the functionals $E^{X}(\rho)$ and $E^{C}(\rho)$ can be found in the literature [34]. Becke introduced a gradient-corrected functional $E^{X}(B)(\rho,\nabla\rho)$ and formulated functionals which include a mixture (hybrid) of Hartree-Fock (HF) exchange and DFT exchange (X) plus correlation (C) as

$$E^{XC}(\text{hybrid}) = c_{HF}E^{X}(\text{HF}) + c_{DFT}E^{XC}(\text{DFT})$$

where the coefficients c are adjustable parameters. Becke's B3LYP functional, for instance, is a three parameter functional of the following composition:

$$E^{XC}(\text{B3LYP}) = E^{X} + c_0[E^{X}(\text{HF}) - E^{X}(\text{DFT})] + c_X E^{X}(\text{B}) + E^{C}(\text{VWN3}) + c_C[E^{C}(\text{LYP}) - E^{C}(\text{VWN3})]$$

where VWN is the Vosko, Wilk, Nusair functional [35], and LYP is the Lee, Yang, Parr functional [36]. The parameters c_0, c_X and c_C are determined by fitting to automization

energies, ionization energies, proton affinities and atomic energies of a set of molecules. Thus, the B3LYP procedure is semi-empirical in this sense. DFT calculations proceed in the same way as *ab initio* HF calculations, with the addition of the extra term E^{XC}, which is computed via numerical integration.

A geometry optimization is complete when the force between the nuclei is below the cutoff value of 0.00045 $E_h a_o^{-1}$, and the calculated displacement of the internuclear distance for the next optimization step is below 0.0018 a_o. For weakly bound systems, scanning of the energy curve was applied in addition.

Vibrational wave number depend on second derivatives of the energy with respect to the nuclear positions. Analytical second derivative are available for DFT calculations. The absolute absorption intensity A which is measured in the unit of mol^{-1} is calculated by the formula

$$A_{1\text{-}0} = (8\pi^3/3hc)N_A \left|\mu_{1-0}\right| \omega_{1-0}$$

where N_A is the Avogadro constant, $\mu_{1\text{-}0}$ is the electric dipole transition moment between the states 0 and 1, and $\omega_{1\text{-}0}$ is the wave number. In the experimental literature, the quantity $S = A/RT$ which is measured in the unit of $cm^{-2}atm^{-1}$ at a given temperature T is used for gases. This quantity results from substitution of the concentration c in Beer's law by the partial pressure p. The conversion of unit is given above.

The structures of Sal_2trien, $ZnSal_2$trien, Sal_2(OMe)trien, $ZnSal_2$(OMe)trien, Sal_2(OEt)trien and $ZnSal_2$(OEt)trien, were optimized by Density Functional Theory (DFT) calculations using 6-31G(d) basis set. The structural energies of Sal_2trien, Sal_2(OMe)trien, Sal_2(OEt)trien and their zinc complexes were computed at B3LYP/6-31G(d) level. All structure optimizations and energy calculations were performed with the GAUSSINT 03 program and graphically interfaced and facilitated by the MOLDEN 3.7 program.

CHAPTER IV

RESULTS AND DISCUSSION

4.1 Synthesis of hexadentate Schiff base metal complexes

Hexadentate schiff base metal complexes were synthesized using the procedure described in the literature [8-9]. The reaction between salicylaldehyde derivatives and metal (II) acetate in methanol formed a template intermediate. Subsequently, the solution of triethylenetetramine was then added to obtain metal complexes (Scheme 4.1).

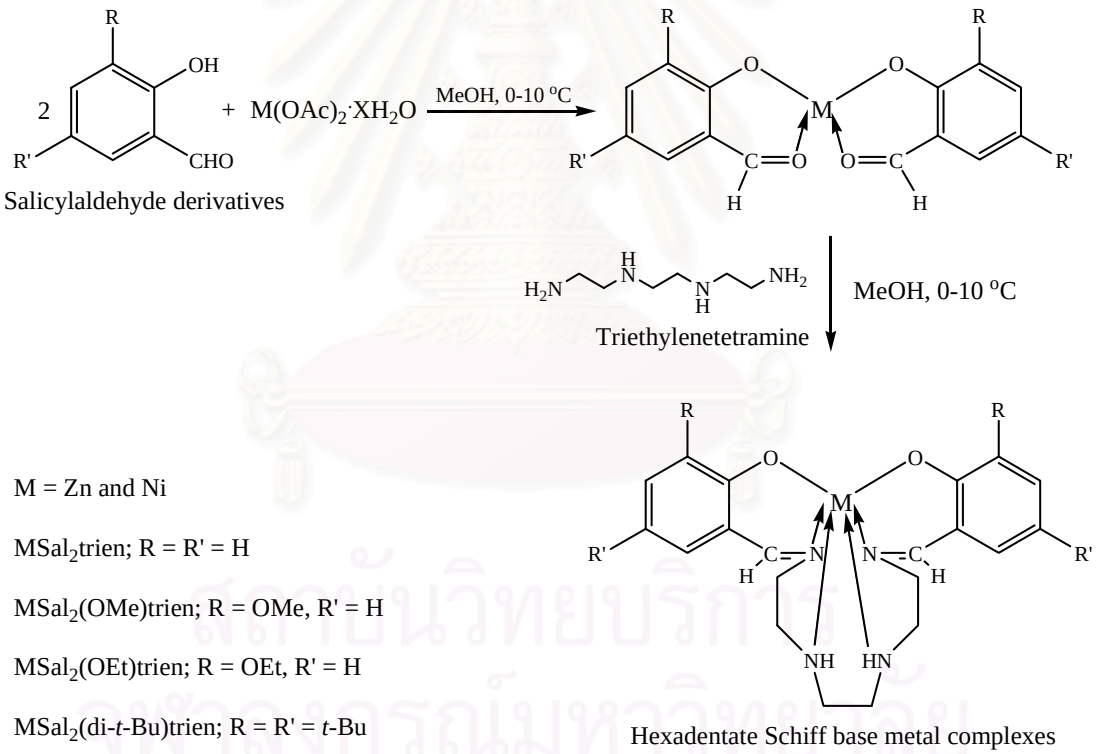

Scheme 4.1 Synthesis of Schiff base metal complexes.

Structures of $ZnSal_2$trien, $ZnSal_2$(OMe)trien, $ZnSal_2$(OEt)trien and $ZnSal_2$(di-*t*-Bu)trien were confirmed by IR and NMR. The spectroscopic data of hexadentate Schiff base zinc complexes were in good agreement with the data reported in the literature [8-9]. IR spectra of zinc complexes shows important bands of C=N stretching

between 1632 and 1648 cm^{-1}. ^{1}H NMR spectra shows the imine -C*H*=N- proton of zinc complexes around 8.13-8.23 ppm.

The structure of $ZnSal_2$trien and $ZnSal_2$(OMe)trien were determined by X-ray crystallography. The crystal structures of $ZnSal_2$trien and $ZnSal_2$(OMe)trien are shown in Figures 4.1 and 4.2, respectively. Both $ZnSal_2$trien and $ZnSal_2$(OMe)trien have roof-shaped structure with the slope containing benzene rings and the zinc atom that adopts a distorted octahedral geometry.

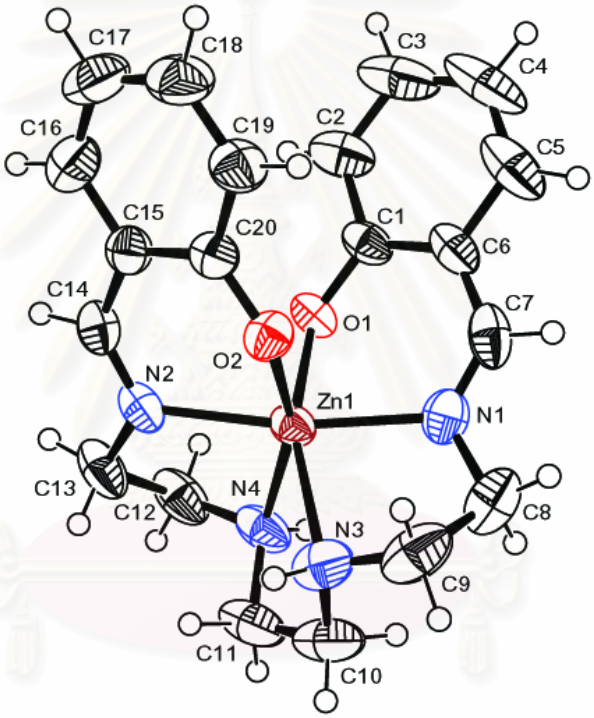

Figure 4.1 X-ray crystal structure of $ZnSal_2$trien.

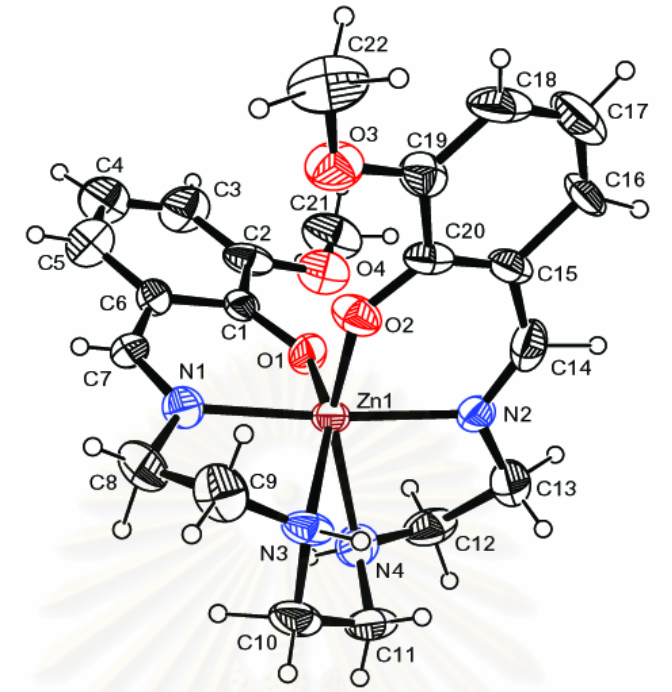

Figure 4.2 X-ray crystal structure of $ZnSal_2$(OMe)trien.

IR spectrum of $NiSal_2$trien shows an absorption band of imine C=N stretching at 1642 cm^{-1} and aromatic C-H bending at 950 cm^{-1}. IR spectra of $NiSal_2$(OMe)trien, $NiSal_2$(OEt)trien and $NiSal_2$(di-*t*-Bu)trien showed an absorption band of imine C=N stretching at 1632, 1648 and 1633 cm^{-1}, respectively. These data agree with those reported in the literature [8-9].

4.2 Protonation constants by potentiometric measurements

The main goals of this research are to refine the protonation constants and stability constants for Schiff base ligands and Schiff base metal complexes, respectively. In general, the stability constants were studied by synthesis of ligand and pH value was adjusted for binding with metal ion. In this research, Schiff base ligands could not be synthesized because it is unstable, therefore Schiff base metal complexes were employed instead of the ligands. Stability constant was studied using Schiff base metal complexes as starting materials. When excess acid (0.05 M $HClO_4$) was added to the metal complex, the metal ion is removed from the metal complex and Schiff base ligand (LH_2) is obtained. The ligand then binds with proton to give Schiff base ligand

cation (LH_4^{2+}). Subsequently, Schiff base ligand cation (LH_4^{2+}) was converted to Schiff base ligand anion (L^{2-}) by addition of tetrabutylammonium hydroxide (Bu_4NOH). Schiff base ligand anion can then form complex with metal ion to give Schiff base metal complexes (Scheme 4.2).

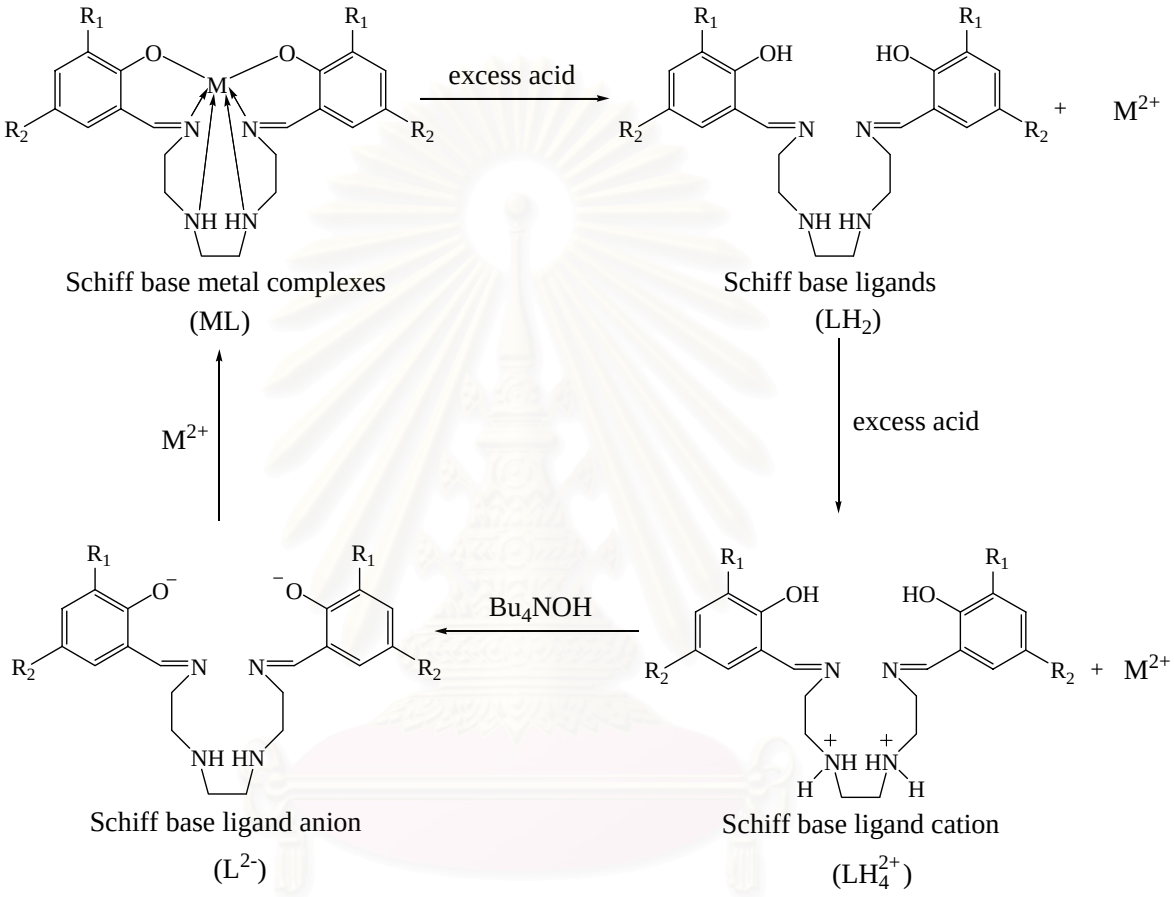

Scheme 4.2 Step of Schiff base complexes formation.

The investigation of proton binding ability of Schiff base ligands were determined by potentiometric technique. The Schiff base ligand cation (LH_4^{2+}) was titrated with tetrabutylammonium hydroxide (Bu_4NOH). The fully protonated form of the Schiff base ligand (Schiff base ligand cation, LH_4^{2+}) can release four protons: two from the secondary amine groups and two from the phenoxyl groups. The titration of Schiff base ligand cation (LH_4^{2+}) with bases can be written as follows:

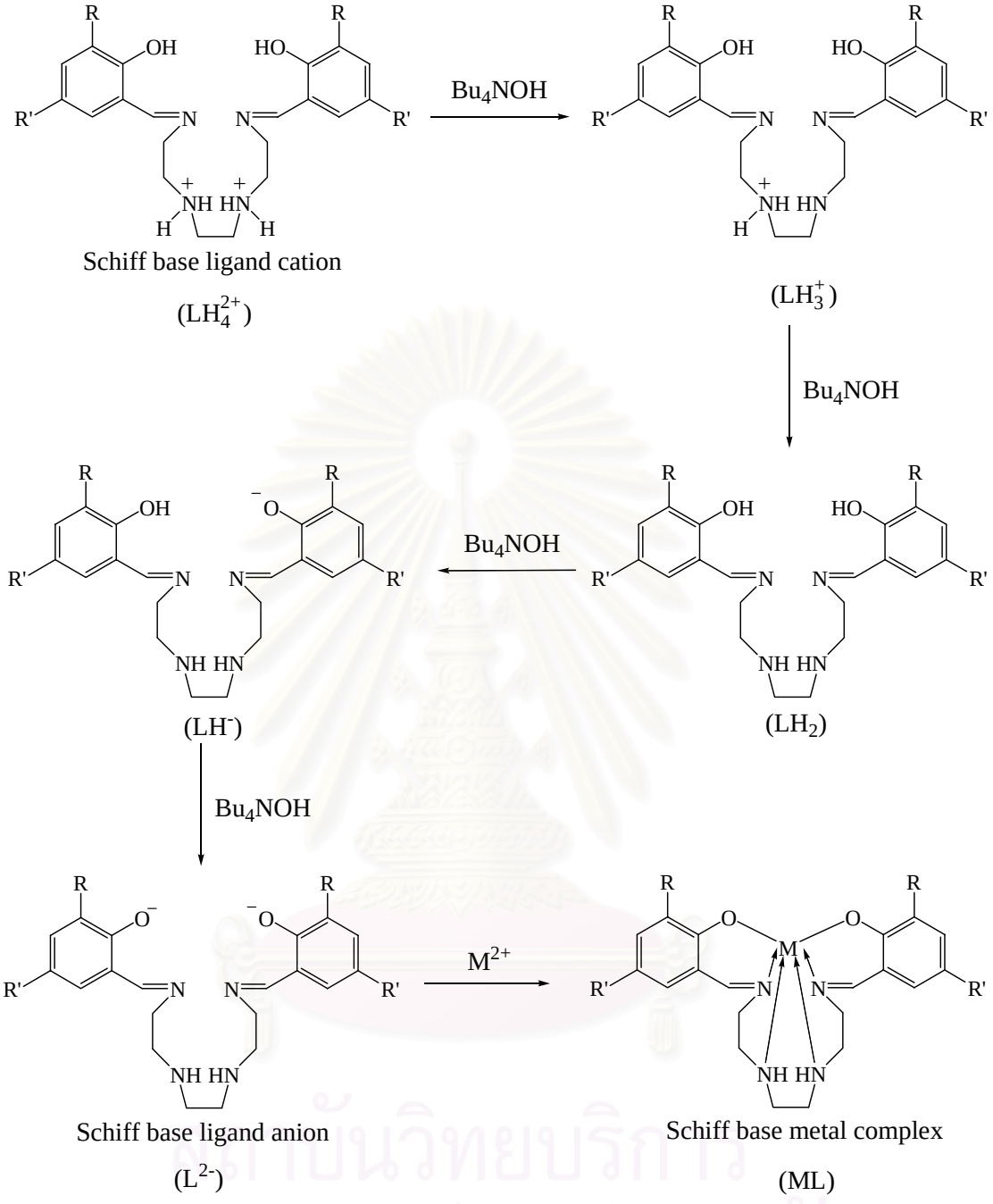

Potentiometric titration was employed to investigate the basicity and complexation abilities of Schiff base metal complexes and their derivatives. At least 40 data points from each titration were used for computer refinement in order to obtain protonation constants and stability constants for metal complexes, which were evaluated by the program SUPERQUAD. The values of protonation constants were calculated by SUPERQUAD program with the chi-square value less than 12.60 in order to 95% confidence.

4.3 Hexadentate Schiff base zinc complexes

4.3.1 $ZnSal_2trien$

The fully protonated species is designated as LH_4^{2+} and the fully deprotonated species as L^{2-}. Log K_n^H values of forth successive stepwise protonation constants of the ligand are shown in Table 4.1. The stepwise protonation constants of each ligand could be calculated as follows:

$$K_n^H = \frac{[H_nL^{(n-2)+}]}{[H_{n-1}L^{(n-3)+}][H]}, \quad n = 1, 2, 3 \text{ and } 4 \qquad (4.1)$$

Table 4.1 Protonation constants of Sal_2trien, (L^{2-}).

Stepwise protonation constants	Log *K*
$L^{2-} + H^+ \rightleftharpoons LH^-$	11.44 ± 0.07
$LH^- + H^+ \rightleftharpoons LH_2$	8.40 ± 0.07
$LH_2 + H^+ \rightleftharpoons LH_3^+$	5.02 ± 0.11
$LH_3^+ + H^+ \rightleftharpoons LH_4^{2+}$	4.92 ± 0.05
$L^{2-} + Zn^{2+} \rightleftharpoons ZnL$	4.56 ± 0.05

Species distribution curves of Sal_2trien, L^{2-}, and its complexes, $ZnSal_2trien$, in 1.00 x 10^{-2} M $Bu_4NCF_3SO_3$ in methanol at 25 ^oC, with complex concentration of 7.685 x 10^{-4} M are shown in Figure 4.3.

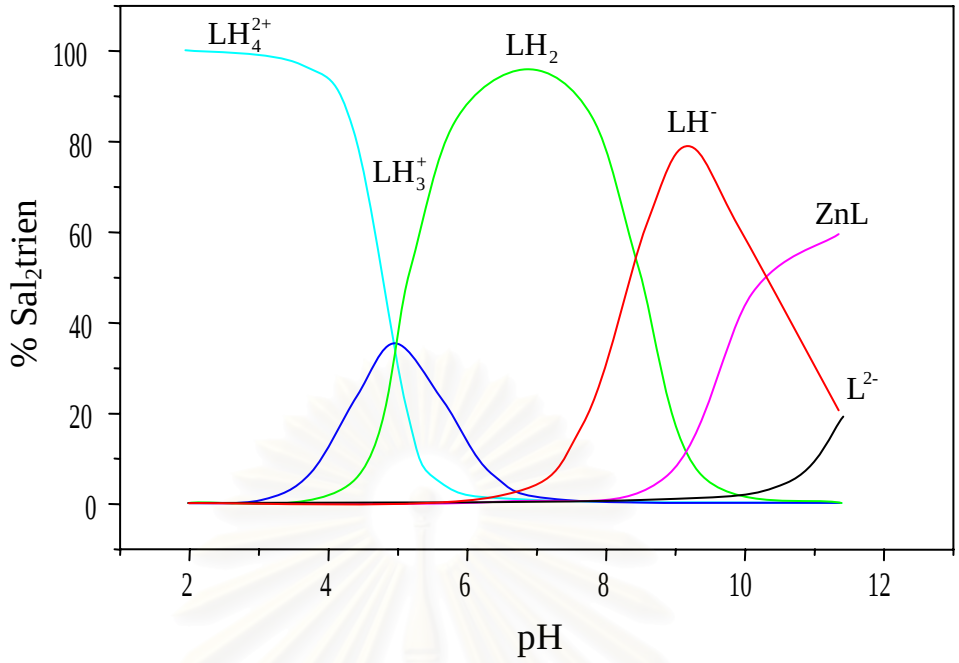

Figure 4.3 Species distribution plot of Sal_2trien (L^{2-}) and $ZnSal_2trien$ (ZnL) in 1.00 x 10^{-2} M $Bu_4NCF_3SO_3$ in methanol at 25 ^oC, C_{ZnL} = 7.685 x 10^{-4} M.

When the pH < 3.0, the ligand exists in the fully protonated form LH_4^{2+}. The last two constants and the first two constants, corresponding to two amino groups and corresponding to two phenolic groups, respectively, are determined by atomic charges of binding atom (Table 4.2). As the pH is increased, the ligand loses its protons from amino nitrogens to become LH_3^+ and LH_2 species respectively. The neutral ligand LH_2 reaches its maximum concentration at pH 7.0 (~95 %). $ZnSal_2trien$ complex (ZnL) is presented at pH above 8.0 and increases while pH in increased.

Table 4.2 Atomic charges of binding atoms in free forms of Sal_2trien, Sal_2(OMe)trien, Sal_2(OEt)trien and their complexing forms with Zn^{2+} ion.

Atom	Mulliken					
	Sal_2trien	$ZnSal_2$trien	Sal_2(OMe)trien	$ZnSal_2$(OMe)trien	Sal_2(OEt)trien	$ZnSal_2$(OEt)trien
O1	-0.614	-0.700	-0.620	-0.690	-0.615	-0.689
O2	-0.614	-0.700	-0.613	-0.685	-0.616	-0.689
O3	-	-	-0.560	-0.485	-0.549	-0.503
O4	-	-	-0.558	-0.486	-0.549	-0.503
N1	-0.367	-0.487	-0.366	-0.487	-0.367	-0.485
N2	-0.367	-0.487	-0.369	-0.490	-0.367	-0.485
N3	-0.593	-0.608	-0.594	-0.612	-0.596	-0.612
N4	-0.593	-0.608	-0.590	-0.612	-0.595	-0.612
Dipole moment, D	1.4462	7.2321	2.9516	5.5705	1.8920	5.6294

4.3.2 $ZnSal_2(OMe)trien$

Log K_n^H values of forth successive stepwise protonation constants of the ligand are shown in Table 4.3.

Table 4.3 Protonation constants of $Sal_2(OMe)trien$, (L^{2-}).

Stepwise protonation constants	Log *K*
$L^{2-} + H^+ \rightleftharpoons LH^-$	11.10 ± 0.04
$LH^- + H^+ \rightleftharpoons LH_2$	8.61 ± 0.04
$LH_2 + H^+ \rightleftharpoons LH_3^+$	5.50 ± 0.04
$LH_3^+ + H^+ \rightleftharpoons LH_4^{2+}$	4.80 ± 0.05
$L^{2-} + Zn^{2+} \rightleftharpoons ZnL$	4.30 ± 0.11

Species distribution curves of $Sal_2(OMe)trien$, L^{2-}, and its complexes, $ZnSal_2(OMe)trien$, in 1.00 x 10^{-2} M $Bu_4NCF_3SO_3$ in methanol at 25 °C, with complex concentration of 8.325 x 10^{-4} M are shown in Figure 4.4.

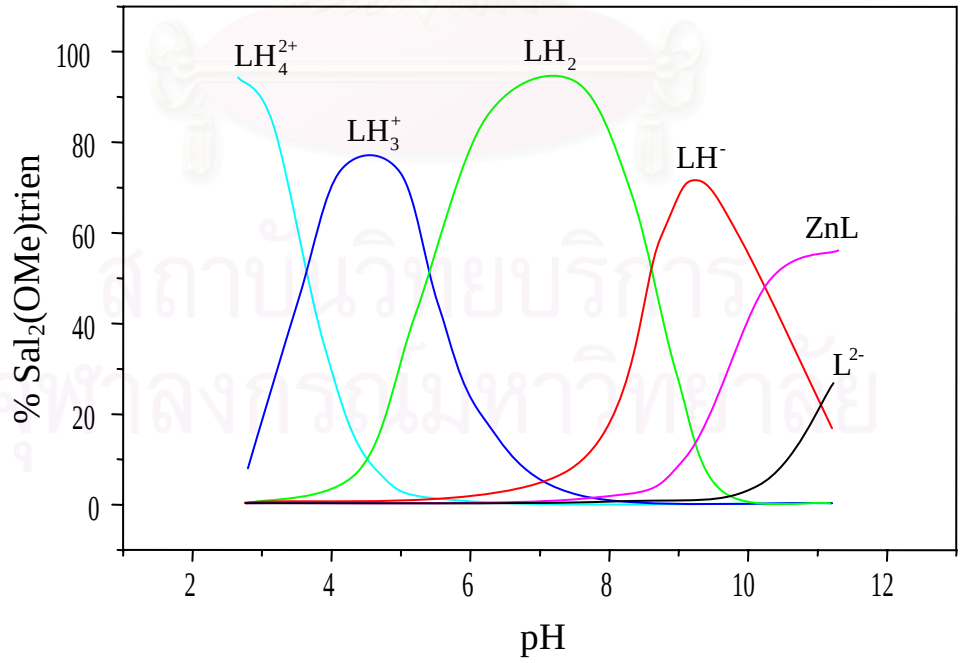

Figure 4.4 Species distribution plot of $Sal_2(OMe)trien$ (L^{2-}) and $ZnSal_2(OMe)trien$ (ZnL) in 1.00 x 10^{-2} M $Bu_4NCF_3SO_3$ in methanol at 25 °C, C_{ZnL} = 8.325 x 10^{-4} M.

When the pH < 2.5, the ligand exists in the fully protonated form LH_4^{2+}. The neutral ligand LH_2 reaches its maximum concentration at pH 7.0 (~95 %). $ZnSal_2$(OMe)trien complex (ZnL) is presented at pH above 9.0 and increases while pH in increased.

4.3.3 $ZnSal_2$(OEt)trien

Log K_n^H values of forth successive stepwise protonation constants of the ligand are shown in Table 4.4.

Table 4.4 Protonation constants of Sal_2(OEt)trien, (L^{2-}).

Stepwise protonation constants	Log *K*
$L^{2-} + H^+ \rightleftharpoons LH^-$	11.37 ± 0.04
$LH^- + H^+ \rightleftharpoons LH_2$	8.50 ± 0.04
$LH_2 + H^+ \rightleftharpoons LH_3^+$	5.51 ± 0.04
$LH_3^+ + H^+ \rightleftharpoons LH_4^{2+}$	4.59 ± 0.05
$L^{2-} + Zn^{2+} \rightleftharpoons ZnL$	3.76 ± 0.09

Species distribution curves of Sal_2(OEt)trien, L^{2-}, and its complexes, $ZnSal_2$(OEt)trien, in 1.00 x 10^{-2} M $Bu_4NCF_3SO_3$ in methanol at 25 ^oC, with complex concentration of 9.091 x 10^{-4} M are shown in Figure 4.5.

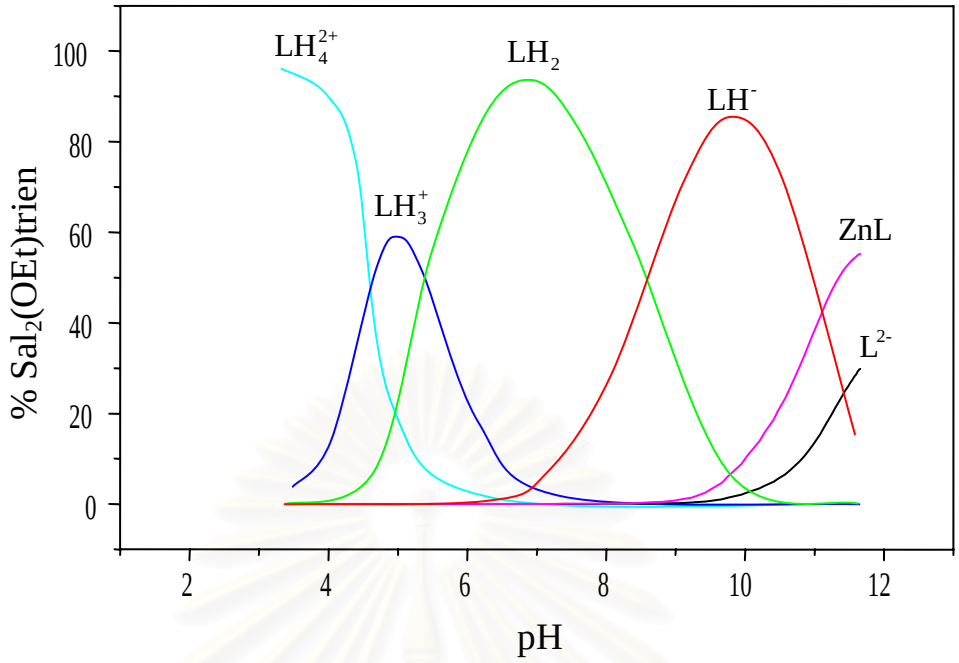

Figure 4.5 Species distribution plot of Sal_2(OEt)trien (L^{2-}) and $ZnSal_2$(OEt)trien (ZnL) in 1.00 x 10^{-2} M $Bu_4NCF_3SO_3$ in methanol at 25 ^oC, C_{ZnL} = 9.091 x 10^{-4} M.

When the pH < 3.0, the ligand exists in the fully protonated form LH_4^{2+}. The neutral ligand LH_2 reaches its maximum concentration at pH 6.8 (~95 %). $ZnSal_2$(OEt)trien complex (ZnL) is presented at pH above 9.5 and increases while pH in increased.

4.4 Hexadentate Schiff base nickel complexes

4.4.1 $NiSal_2$trien

Log K_n^H values of forth successive stepwise protonation constants of the ligand are shown in Table 4.5.

Table 4.5 Protonation constants of Sal_2trien, (L^{2-}).

Stepwise protonation constants	Log *K*
$L^{2-} + H^{+} \rightleftharpoons LH^{-}$	11.19 ± 0.05
$LH^{-} + H^{+} \rightleftharpoons LH_2$	7.67 ± 0.02
$LH_2 + H^{+} \rightleftharpoons LH_3^{+}$	6.70 ± 0.05
$LH_3^{+} + H^{+} \rightleftharpoons LH_4^{2+}$	4.12 ± 0.05
$L^{2-} + Ni^{2+} \rightleftharpoons NiL$	4.80 ± 0.17

Species distribution curves of Sal_2trien, L^{2-}, and its complexes, $NiSal_2trien$, in 1.00 x 10^{-2} M $Bu_4NCF_3SO_3$ in methanol at 25 ^{o}C, with complex concentration of 9.505 x 10^{-4} M are shown in Figure 4.6.

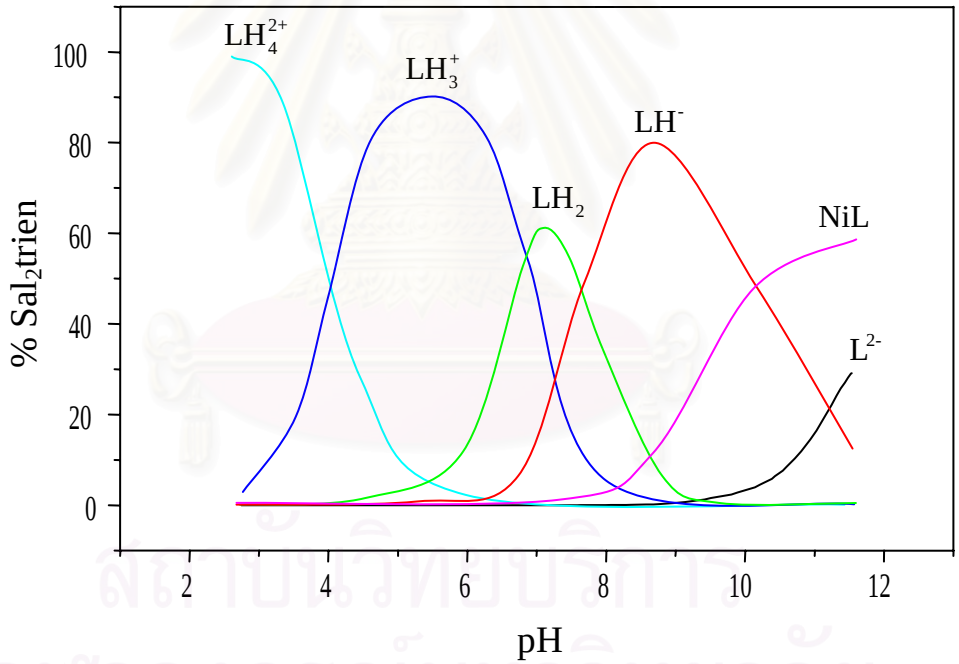

Figure 4.6 Species distribution plot of Sal_2trien (L^{2-}) and $NiSal_2trien$ (NiL) in 1.00 x 10^{-2} M $Bu_4NCF_3SO_3$ in methanol at 25 ^{o}C, C_{NiL} = 9.505 x 10^{-4} M.

When the pH < 2.5, the ligand exists in the fully protonated form LH_4^{2+}. The neutral ligand LH_2 reaches its maximum concentration at pH 7.2 (~60 %). $NiSal_2trien$ complex (NiL) is presented at pH above 8.5 and increases while pH in increased.

4.4.2 $NiSal_2(OMe)trien$

Log K_n^H values of forth successive stepwise protonation constants of the ligand are shown in Table 4.6.

Table 4.6 Protonation constants of $Sal_2(OMe)trien$, (L^{2-}).

Stepwise protonation constants	Log *K*
$L^{2-} + H^+ \rightleftharpoons LH^-$	11.28 ± 0.12
$LH^- + H^+ \rightleftharpoons LH_2$	8.05 ± 0.13
$LH_2 + H^+ \rightleftharpoons LH_3^+$	4.94 ± 0.13
$LH_3^+ + H^+ \rightleftharpoons LH_4^{2+}$	3.36 ± 0.15
$L^{2-} + Ni^{2+} \rightleftharpoons NiL$	5.77 ± 0.14

Species distribution curves of $Sal_2(OMe)trien$, L^{2-}, and its complexes, $NiSal_2(OMe)trien$, in 1.00 x 10^{-2} M $Bu_4NCF_3SO_3$ in methanol at 25 °C, with complex concentration of 8.317 x 10^{-4} M are shown in Figure 4.7.

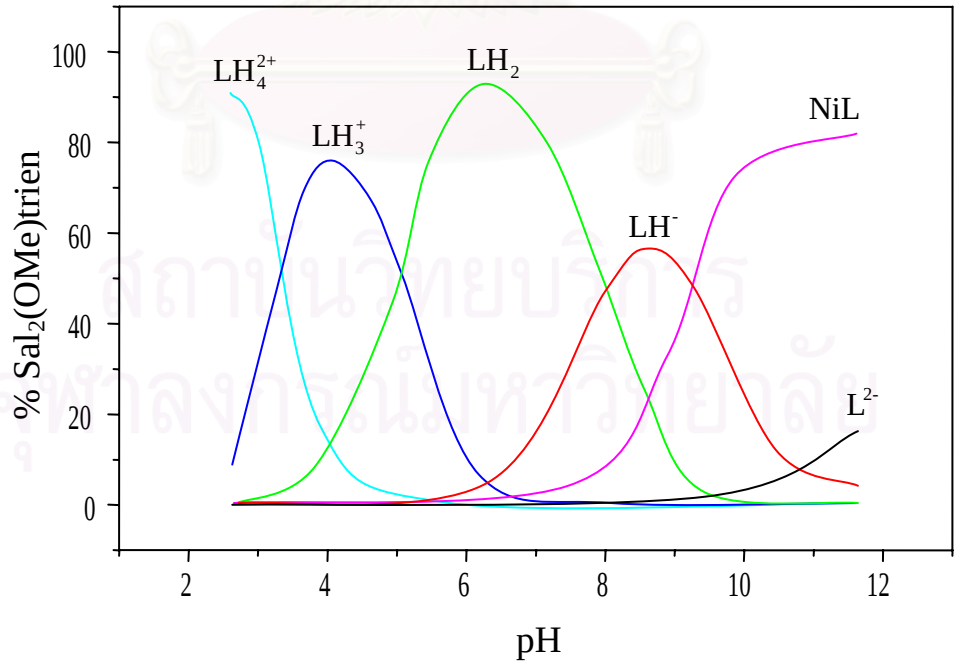

Figure 4.7 Species distribution plot of $Sal_2(OMe)trien$ (L^{2-}) and $NiSal_2(OMe)trien$ (NiL) in 1.00 x 10^{-2} M $Bu_4NCF_3SO_3$ in methanol at 25 °C, C_{NiL} = 8.317 x 10^{-4} M.

When the pH < 2.5, the ligand exists in the fully protonated form LH_4^{2+}. The neutral ligand LH_2 reaches its maximum concentration at pH 6.2 (~90 %). $NiSal_2$(OMe)trien complex (NiL) is presented at pH above 8.0 and increases while pH in increased.

4.4.3 $NiSal_2$(OEt)trien

Log K_n^H values of forth successive stepwise protonation constants of the ligand are shown in Table 4.7.

Table 4.7 Protonation constants of Sal_2(OEt)trien, (L^{2-}).

Stepwise protonation constants	Log *K*
$L^{2-} + H^+ \rightleftharpoons LH^-$	12.21 ± 0.03
$LH^- + H^+ \rightleftharpoons LH_2$	7.71 ± 0.02
$LH_2 + H^+ \rightleftharpoons LH_3^+$	5.09 ± 0.02
$LH_3^+ + H^+ \rightleftharpoons LH_4^{2+}$	3.67 ±0.03
$L^{2-} + Ni^{2+} \rightleftharpoons NiL$	7.08 ± 0.03

Species distribution curves of Sal_2(OEt)trien, L^{2-}, and its complexes, $NiSal_2$(OEt)trien, in 1.00 x 10^{-2} M $Bu_4NCF_3SO_3$ in methanol at 25 ^oC, with complex concentration of 8.333 x 10^{-4} M are shown in Figure 4.8.

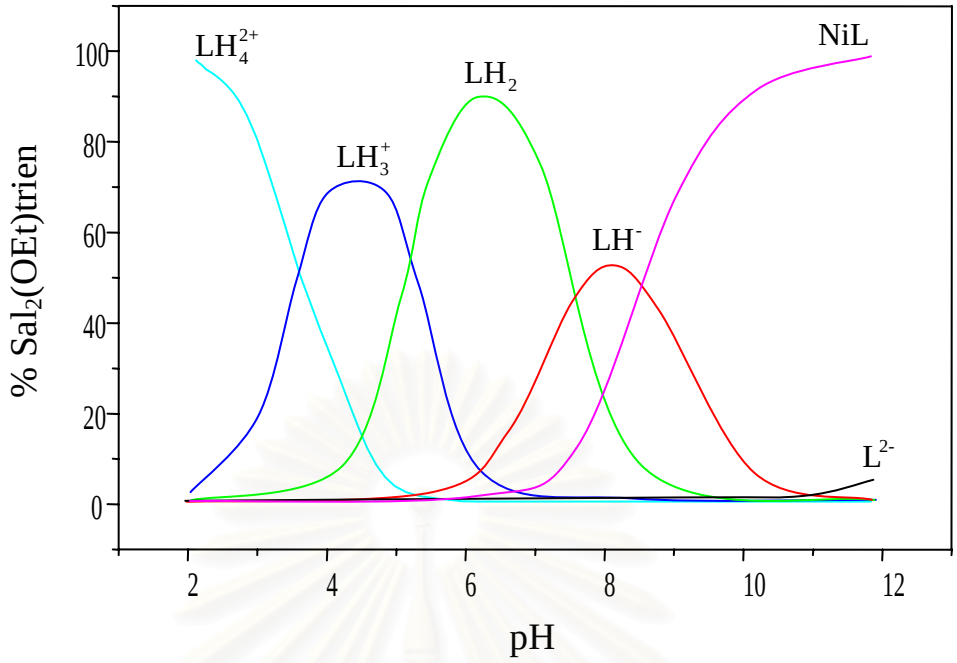

Figure 4.8 Species distribution plot of Sal_2(OEt)trien (L^{2-}) and $NiSal_2$(OEt)trien (NiL) in 1.00 x 10^{-2} M $Bu_4NCF_3SO_3$ in methanol at 25 ^oC, C_{NiL} = 8.333 x 10^{-4} M.

When the pH < 2.0, the ligand exists in the fully protonated form LH_4^{2+}. The neutral ligand LH_2 reaches its maximum concentration at pH 6.2 (~90 %). $NiSal_2$(OEt)trien complex (NiL) is presented at pH above 7.5 and increases while pH in increased.

Comparing between the protonation constants obtained from $ZnSal_2$trien and $NiSal_2$trien (Tables 4.1 and 4.5, respectively), the obtained protonation constants of Sal_2trien in each step are different. In fact, these values should be the same since they were the data of the same ligand, Sal_2trien. The stepwise protonation constants of the ligands Sal_2(OMe)trien, which were obtained from $ZnSal_2$(OMe)trien and $NiSal_2$(OMe)trien (Tables 4.3 and 4.6, respectively), and Sal_2(OEt)trien, which were obtained from $ZnSal_2$(OEt)trien and $NiSal_2$(OEt)trien (Tables 4.4 and 4.7, respectively), also show the same trend as in the case of Sal_2trien. This might be because of the metal ion presented in the solution during titration process (Zn^{2+} and Ni^{2+}) are different.

Since $ZnSal_2$(di-*t*-Bu)trien and $NiSal_2$(di-*t*-Bu)trien are very sensitive to acid. They could be hydrolyzed in acid solution and converted to starting materials as shown in Scheme 4.3.

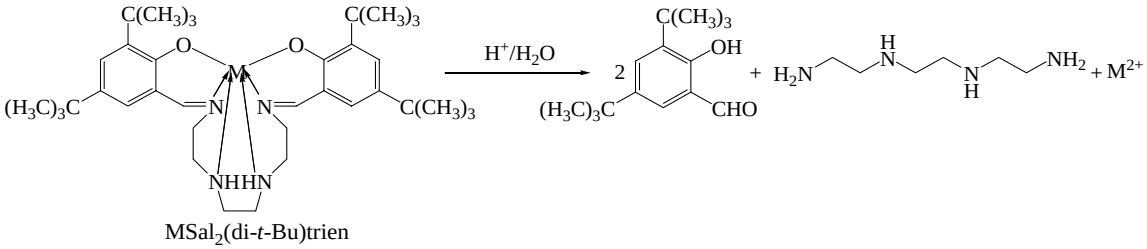

$MSal_2$(di-*t*-Bu)trien

M = Zn and Ni

Scheme 4.3 Proposed hydrolysis of $MSal_2$(di-*t*-Bu)trien in acid solution.

Titration curve of $NiSal_2$(di-*t*-Bu)trien is sigmoidal type (Figure 4.9) which might result from the reaction between 3,5-di-*tert*-butyl-2-hydroxybenzaldehyde and tetrabutylammonium hydroxide.

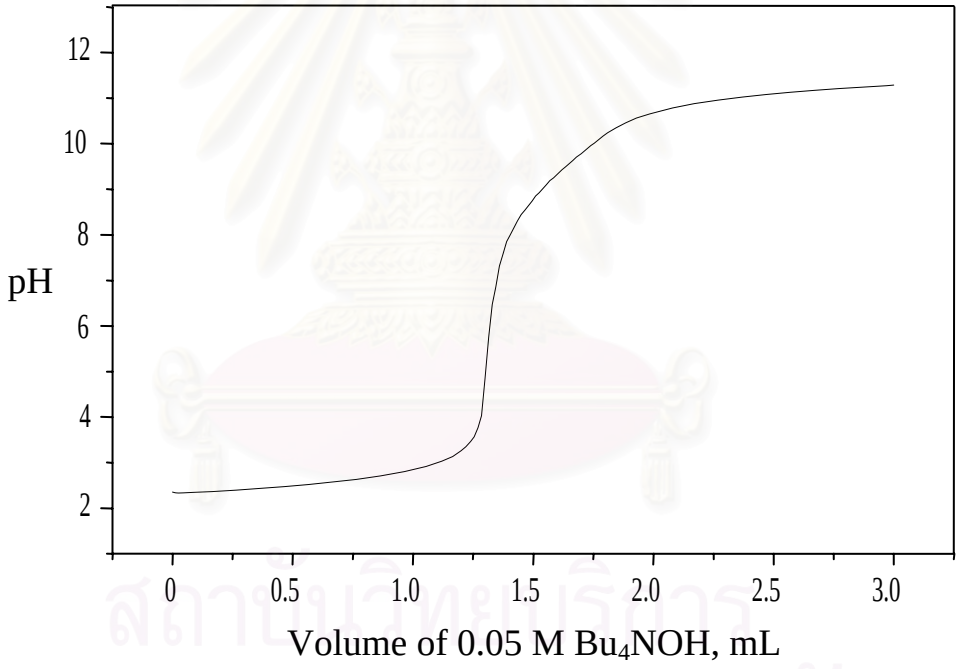

Figure 4.9 Titration curve of 9.081 x 10^{-4} M $NiSal_2$(di-*t*-Bu)trien with 5.00 x 10^{-2} M tetrabutylammonium hydroxide.

4.5 Stability constants by potentiometric measurements

Stability constants of zinc and nickel complexes expressed in terms of overall logarithmic value (log β) are summarized in Table 4.8. Considering the log β values of metal complexes, it could be seen that the stability constants of nickel complexes are

higher than those of zinc complexes which indicates that nickel complexes are more stable than zinc complexes. Since the electron configurations of nickel(II) and zinc(II) ions are $[Ar]3d^6 4s^2$ and $[Ar]3d^8 4s^2$, respectively, nickel(II) ion has more ability in forming the complexes with hexadentate Schiff base ligands than zinc(II) ion.

Table 4.8 Stability constants of zinc and nickel complexes in 1.00 x 10^{-2} M $Bu_4NCF_3SO_3$ in methanol at 25 ^oC.

Metal complexes	Stability constants of metal complexes (log β)	
	Zn	Ni
$MSal_2$trien	4.56 ± 0.05	4.80 ± 0.17
$MSal_2$(OMe)trien	4.30 ± 0.11	5.77 ± 0.14
$MSal_2$(OEt)trien	3.76 ± 0.09	7.08 ± 0.03

This result corresponds to the Irving-William sequence [37], which describes that the order of stability constants for metal complexes from different cations is Cu^{2+} , $Ni^{2+} > Zn^{2+}$. For example, the stability constant data of the metal complexes derived from the ligands 1,2,3-triaminopropane and *N*-(2-aminoethyl)ethylenediamine (Table 4.9) shows that their nickel complexes are more stable than zinc complexes.

Table 4.9 Stability constants for 1,2,3-triaminopropane and *N*-(2-aminoethyl)ethylenediamine complexes of transition metals (measured at 20 ^oC in an aqueous medium 0.1 M in KCl).

Ligand	Metal			
	Co^{2+}	Ni^{2+}	Cu^{2+}	Zn^{2+}
1,2,3-triaminopropane	6.8	9.3	11.1	6.75
N-(2-aminoethyl)ethylenediamine	8.1	10.7	16.0	8.9

When consider the log β values of metal complexes (Table 4.8), the stability constants of nickel complexes increase when the complexes have the electron donating group, CH_3O- and C_2H_5O-, on the aromatic ring. This could be explained by electronic

effect of substituted group on the aromatic ring. Electron density is found at ortho-para positions which directly effect to phenolic oxygen. As a result, the phenolic oxygen has more electrons which lead to good ability in forming metal complexes. The complex formation of $NiSal_2$(OEt)trien and $NiSal_2$(OMe)trien is better than $NiSal_2$trien which has no electron donating group.

On the other hand, stability constants of zinc complexes decrease when their complexes have CH_3O- and C_2H_5O- as substituents on the aromatic ring since electron configuration of Zn^{2+} is $[Ar]3d^{10}$ (Table 4.10). The zinc complex is thus less stable when coordinates to electron rich ligand.

Table 4.10 Physical properties of elements nickel and zinc [38].

Physical properties	Nickel	Zinc
Atomic number	28	30
Electronic configuration	$[Ar]3d^8 4s^2$	$[Ar]3d^{10}4s^2$
Electronegativity	1.8	1.6
Ionic radius/Å (II)	0.63	0.88
Density (25 ^oC)/g.cm^{-1}	8.908	7.14

4.6 Quantum chemical calculations

The structures of Sal_2trien, $ZnSal_2$trien, Sal_2(OMe)trien, $ZnSal_2$(OMe)trien, Sal_2(OEt)trien and $ZnSal_2$(OEt)trien were optimized by Density Functional Theory (DFT) calculations using 6-31G(d) basis set. Total of thermodynamic energies of Sal_2trien, Sal_2(OMe)trien, Sal_2(OEt)trien and their zinc complexes were computed at B3LYP/6-31G(d) level of theory as listed in Table 4.11.

Table 4.11 Total energies and thermodynamic quantities of Sal_2trien, Sal_2(OMe)trien, Sal_2(OEt)trien and their Zinc complexes were computed at B3LYP/6-31G(d) level of theory.

Species	E (hartree)	H (hartree)	G (hartree)
$ZnSal_2$trien[a]	-2924.837902	-2924.812619	-2924.891744
Sal_2trien[b]	-1145.462847	-1145.441081	-1145.511889
Sal_2trien (free)[c]	-1145.556674	-1145.532799	-1145.610459
$ZnSal_2$(OMe)trien[a]	-3153.806104	-3153.777251	-3153.863213
Sal_2(OMe)trien[b]	-1374.430164	-1374.403030	-1374.485852
Sal_2(OMe)trien (free)[c]	-1374.462645	-1374.436718	-1374.519120
$ZnSal_2$(OEt)trien[a]	-3232.383025	-3232.349792	-3232.447698
Sal_2(OEt)trien[b]	-1453.006106	-1452.976325	-1453.065346
Sal_2(OEt)trien (free)[c]	-1453.120798	-1453.08746	-1453.189007

[a] Species of metal complexes

[b] Species of complexes-form ligand

[c] Species of Schiff base free ligand

$$\Delta E_{binding} = [E_{complex} - E_{isolated\ free\ ligand} - E_{metal}] \quad (4.2)$$

$$\Delta E_{complexation} = [E_{complex} - E_{complex\text{-}form\ ligand} - E_{metal}] \quad (4.3)$$

The above formulas are the binding and complexation model of Schiff base metal complexes. $\Delta E_{binding}$ is the difference in energy of complexes and isolated free ligand and metal. $\Delta E_{complexation}$ is the difference in energy of complexes and complex-form ligand and metal. The difference of isolated free ligand and complex-form ligand is ligand rearrangement. The complex-form ligand immediately form complex with metal ion, but the isolated free ligand will be rearranged structure before they bind metal ion. The difference of energy between complexation and binding energies are called preorganization energy ($\Delta E_{preorganization}$), which could be written as follows:

$$\Delta E_{preorganization} = \Delta E_{complexation} - \Delta E_{binding} \quad (4.4)$$

The corresponding enthalpy, $\Delta H_{binding}$ and Gibbs free energy, $\Delta G_{binding}$ could be written in the same fashion as equation 4.2 as follows:

$$\Delta H_{binding} = [H_{complex} - H_{isolated\ free\ ligand} - H_{metal}] \quad (4.5)$$

$$\Delta G_{binding} = [G_{complex} - G_{isolated\ free\ ligand} - G_{metal}] \quad (4.6)$$

Internal energy of binding of $ZnSal_2$trien, $ZnSal_2$(OMe)trien and $ZnSal_2$(OEt)trien complexes at B3LYP/6-31G(d) level are -736.83, -775.88 and -724.91 kcal/mol as listed in Tables 4.12, 4.13 and 4.14, respectively. This indicates that the order of stability of zinc complexes is $ZnSal_2$(OMe)trien > $ZnSal_2$trien > $ZnSal_2$(OEt)trien.

Table 4.12 Preorganization energies of Sal_2trien, binding and complexation energies of zinc complexes were computed at B3LYP/6-31G(d) level of theory.

Reactions	ΔE (kcal mol^{-1})	ΔH (kcal mol^{-1})	ΔG (kcal mol^{-1})	ΔS (cal mol^{-1} K^{-1})
Binding	-736.83	-737.43	-726.90	-35.30
Complexation	-795.71	-794.98	-788.76	-20.88
Preorganization	58.88	57.55	61.85	-14.42

Table 4.13 Preorganization energies of Sal_2(OMe)trien, binding and complexation energies of zinc complexes were computed at B3LYP/6-31G(d) level of theory.

Reactions	ΔE (kcal mol^{-1})	ΔH (kcal mol^{-1})	ΔG (kcal mol^{-1})	ΔS (cal mol^{-1} K^{-1})
Binding	-775.88	-775.53	-766.32	-30.89
Complexation	-796.26	-796.67	-787.19	-31.78
Preorganization	20.38	21.14	20.88	0.88

Table 4.14 Preorganization energies of Sal_2(OEt)trien, binding and complexation energies of zinc complexes were computed at B3LYP/6-31G(d) level of theory.

Reactions	ΔE (kcal mol^{-1})	ΔH (kcal mol^{-1})	ΔG (kcal mol^{-1})	ΔS (cal mol^{-1} K^{-1})
Binding	-724.91	-726.45	-712.73	-46.05
Complexation	-796.88	-796.19	-790.32	-19.69
Preorganization	71.97	69.74	77.60	-26.36

Preoganization energy of Sal_2(OEt)trien (ΔE_{preorg} = 71.97 kcal/mol) is larger than that of Sal_2trien (ΔE_{preorg} = 58.88 kcal/mol) and Sal_2(OMe)trien (ΔE_{preorg} = 20.38 kcal/mol) by 13.09 and 51.59 kcal/mol, respectively. This result is mainly caused by the repulsion between two ethoxyl groups in Sal_2(OEt)trien since preorganization energy depends on steric effect and hydrogen bond formation. The preorganization energy of Sal_2trien is larger than that of Sal_2(OMe)trien because the intramolecular hydrogen bonding could be only formed in Sal_2trien (Figure 4.10, (a)). Therefore, the rearrangement of Sal_2trien to form complex requires more energy than that in the case of Sal_2(OMe)trien. Sal_2(OMe)trien and Sal_2(OEt)trien cannot form intramolecular hydrogen bonding since a distance between phenolate oxygen ion and hydrogen atom of secondary amine is more than 2.5 Å as shown in Table 4.15.

Table 4.15 Hydrogen bond distance between phenolate oxygen ion and hydrogen atom of secondary amine of Schiff base ligands.

Schiff base ligands	Distance of Ph-O···H-N- (Å) [a]
Sal_2trien	2.5
Sal_2(OMe)trien	> 2.5
Sal_2(OEt)trien	> 2.5

[a] Obtained from molekel 4.3 program

Optimization structures of Sal_2trien, Sal_2(OMe)trien, Sal_2(OEt)trien and their zinc complexes at B3LYP/6-31G(d) level are shown in Figure 4.10.

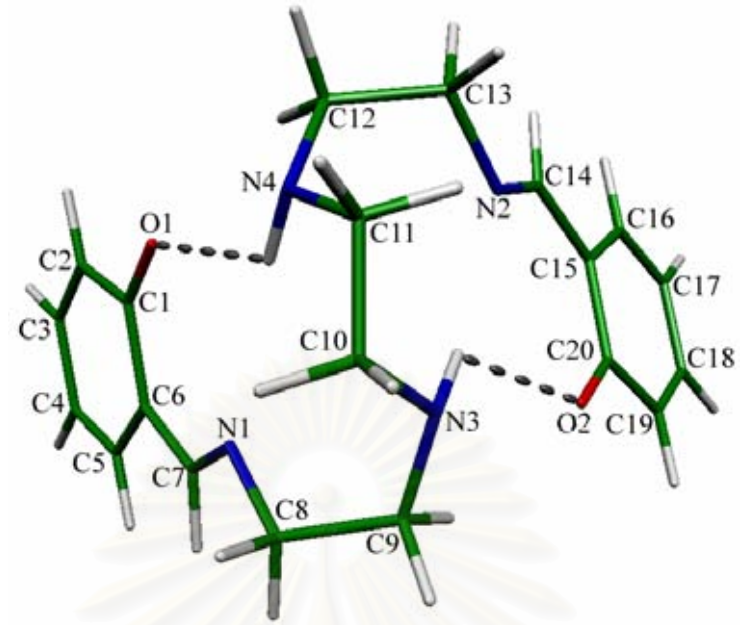

(a)

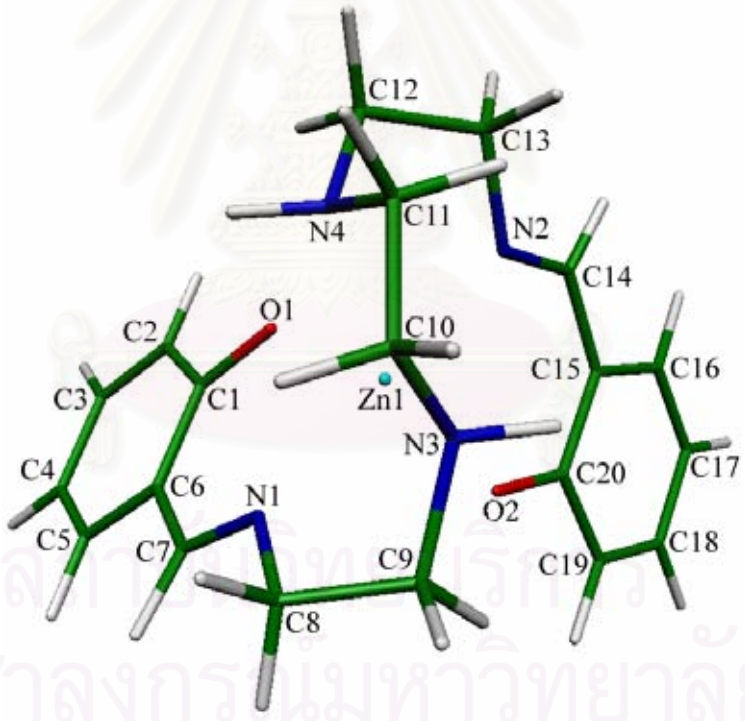

(b)

Figure 4.10 B3LYP/6-31G(d)-optimized structures of (a) free form, (b) complex form of Sal_2trien, (c) free form and (d) complex form of Sal_2(OMe)trien, (e) free form and (f) complex form of Sal_2(OEt)trien.

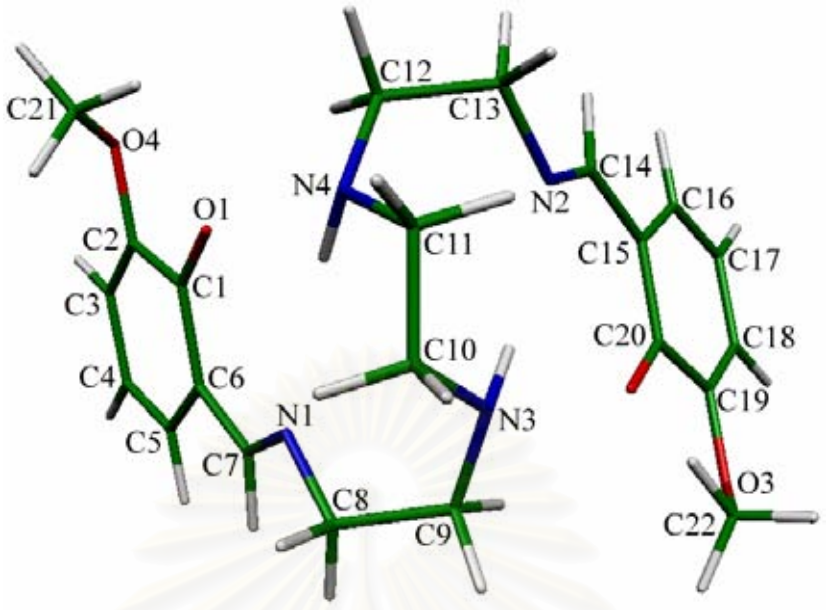

(c)

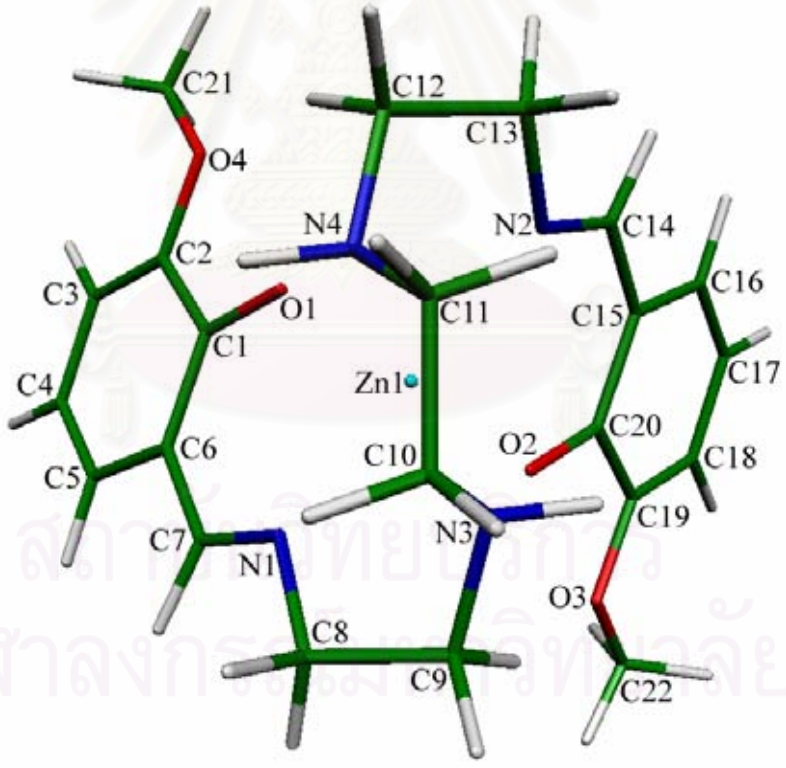

(d)

Figure 4.10 (continued).

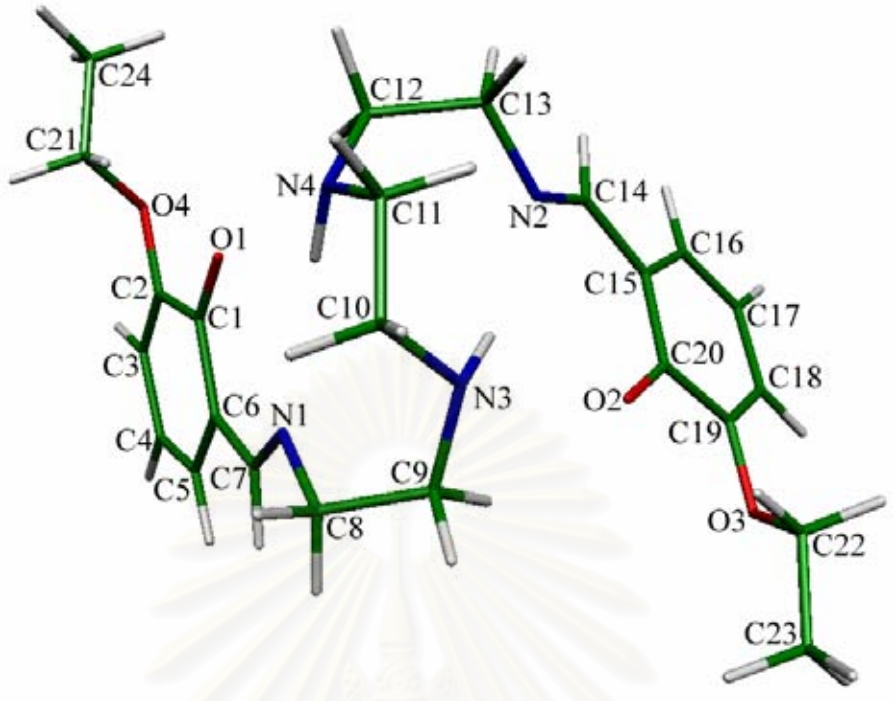

(e)

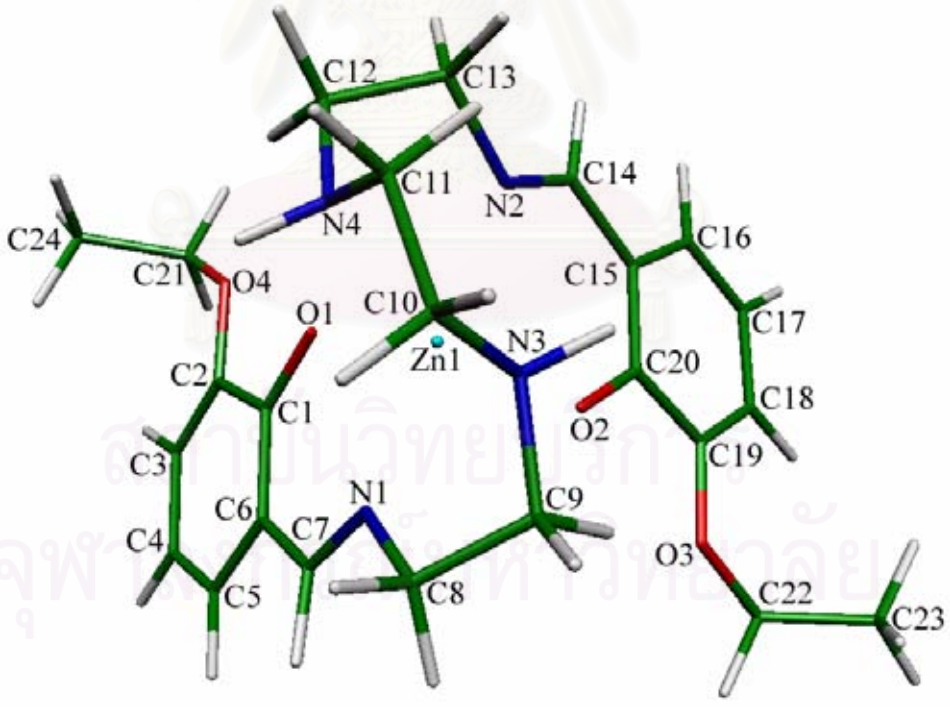

(f)

Figure 4.10 (continued).

Giffs free energies of binding and complexation of zinc complexes are less than zero which indicates that the complex formation could be spontaneous. Although Gibbs free energies of preorganization are more than zero, however, the entropy of preorganization is very low. Since, the rearrangement of molecule is explained by entropy, the complex formation is spontaneous.

Atomic charges of donor atoms in Sal_2trien, Sal_2(OMe)trien, Sal_2(OEt)trien and their zinc complexes are listed in Table 4.2. The order of solubility of zinc complexes in polar organic solvent such as methanol is $ZnSal_2$trien > $ZnSal_2$(OEt)trien > $ZnSal_2$(OMe)trien which correlates to their dipole moment values (Table 4.2).

In the previous work [9], metal-containing polyureas were synthesized from the reaction between hexadentate Schiff base metal complexes and diisocynates (Scheme 4.4) at a mole ratio of 1:1 to avoid cross-linking of the polyureas. The polymerization mechanism is that the -NH- groups in the metal complex undergo a reaction with isocyanate groups to give urea linkages.

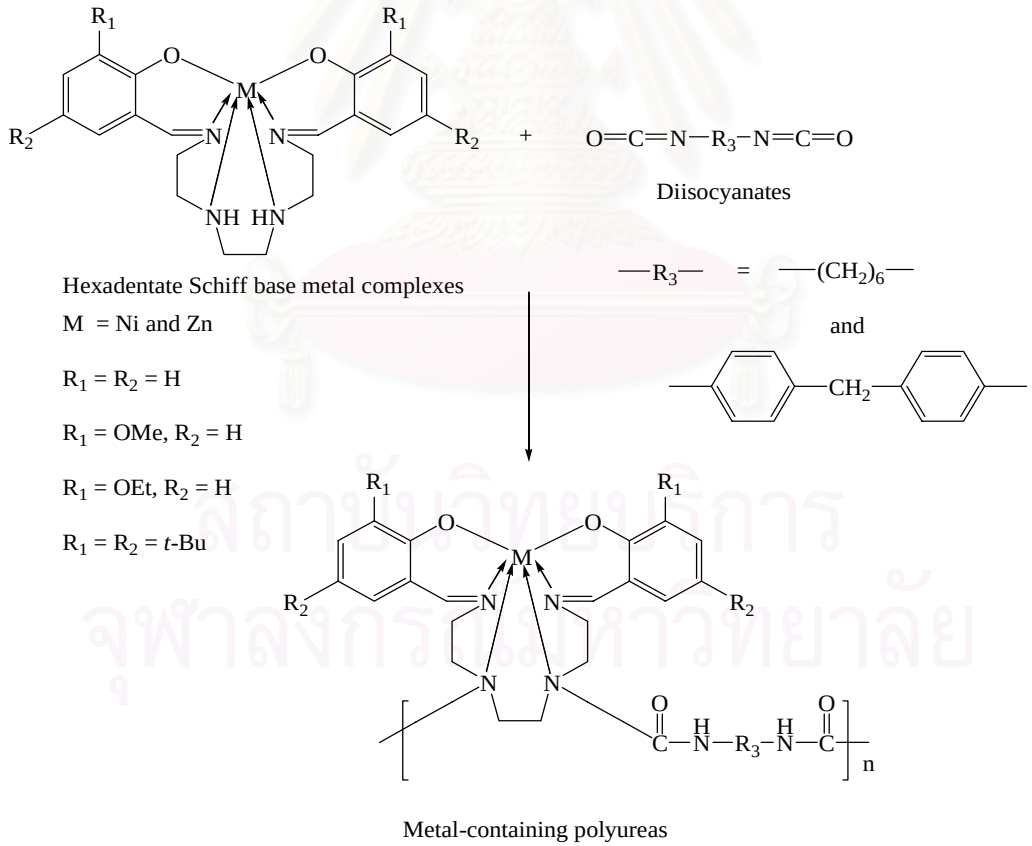

Scheme 4.4 Synthesis of metal-containing polyureas from the reaction between metal complexes and diisocyanates.

The reaction progress could be observed by the disappearance of the strong NCO absorption of diispcyanate at 2270 cm^{-1} and the appearance of a new urea C=O absorption band at 1687-1720 cm^{-1}. The polymerization mechanism is in good agreement with the atomic charges of the -NH- groups (N3 and N4) in the hexadentate Schiff base zinc complexes (Table 4.2). B3LYP/6-31G(d) optimized geometrical data of $ZnSal_2$trien and $ZnSal_2$(OMe)trien are in good agreement with the X-ray crystallographic data [39] as listed in Tables 4.15, 4.16 and 4.17. For $ZnSal_2$(OEt)trien, only the calculated values are reported since the crystal structure of $ZnSal_2$(OEt)trien could not be obtained.

Table 4.16 Bond length data for the structures of $ZnSal_2$trien, $ZnSal_2$(OMe)trien and $ZnSal_2$(OEt)trien.

Bond length (Å)	$ZnSal_2$trien		$ZnSal_2$(OMe)trien		$ZnSal_2$(OEt)trien	
	B3LYP/ 6-31G(d)	Exp.	B3LYP/ 6-31G(d)	Exp.	B3LYP/ 6-31G(d)	Exp.
Zn1-O1	2.009	2.087	2.017	2.063	2.010	-
Zn1-O2	2.009	2.091	2.017	2.055	2.010	-
Zn1-N1	2.130	2.125	2.130	2.147	2.130	-
Zn1-N2	2.130	2.149	2.140	2.146	2.130	-
Zn1-N3	2.310	2.224	2.290	2.295	2.290	-
Zn1-N4	2.310	2.222	2.290	2.228	2.290	-
C1-O1	1.295	1.318	1.280	1.308	1.280	-
C1-C2	1.420	1.414	1.440	1.455	1.440	-
C1-C6	1.440	1.415	1.430	1.492	1.430	-
C2-O4	-	-	1.360	1.340	1.370	-
C2-C3	1.380	1.373	1.380	1.388	1.380	-
C3-C4	1.410	1.380	1.410	1.420	1.410	-
C4-C5	1.380	1.345	1.370	1.419	1.370	-
C5-C6	1.410	1.407	1.420	1.371	1.420	-
C6-C7	1.430	1.440	1.430	1.441	1.440	-
C7-N1	1.296	1.270	1.290	1.290	1.290	-
C8-C9	1.530	1.517	1.530	1.501	1.530	-

Table 4.16 (continued).

Bond length (Å)	$ZnSal_2$trien		$ZnSal_2$(OMe)trien		$ZnSal_2$(OEt)trien	
	B3LYP/ 6-31G(d)	Exp.	B3LYP/ 6-31G(d)	Exp.	B3LYP/ 6-31G(d)	Exp.
C8-N1	1.456	1.467	1.460	1.503	1.450	-
C9-N3	1.470	1.460	1.470	1.485	1.470	-
C10-C11	1.530	1.500	1.530	1.511	1.530	-
C10-N3	1.460	1.484	1.460	1.519	1.460	-
C11-N4	1.460	1.473	1.460	1.458	1.460	-
C12-N4	1.470	1.469	1.470	1.464	1.470	-
C12-C13	1.530	1.526	1.530	1.566	1.530	-
C13-N2	1.450	1.467	1.450	1.433	1.450	-
C14-N2	1.290	1.276	1.290	1.288	1.296	-
C14-C15	1.430	1.441	1.420	1.458	1.430	-
C15-C20	1.440	1.426	1.430	1.367	1.430	-
C15-C16	1.420	1.406	1.420	1.473	1.420	-
C16-C17	1.370	1.365	1.370	1.299	1.370	-
C17-C18	1.410	1.376	1.410	1.402	1.410	-
C18-C19	1.380	1.369	1.380	1.397	1.380	-
C19-O3	-	-	1.360	1.427	1.370	-
C19-C20	1.420	1.418	1.440	1.439	1.440	-
C20-O2	1.290	1.307	1.280	1.291	1.290	-
C21-O4	-	-	1.412	1.417	1.420	-
C22-O3	-	-	1.412	1.427	1.420	-
C21-C24	-	-	-	-	1.520	-
C22-C23	-	-	-	-	1.520	-

Table 4.17 Bond angles data for the structures of $ZnSal_2$trien, $ZnSal_2$(OMe)trien and $ZnSal_2$(OEt)trien.

Bond Angles (°)	$ZnSal_2$trien		$ZnSal_2$(OMe)trien		$ZnSal_2$(OEt)trien	
	B3LYP/ 6-31G(d)	Exp.	B3LYP/ 6-31G(d)	Exp.	B3LYP/ 6-31G(d)	Exp.
C7-C6-C1	122.988	-	122.257	122.8	122.130	-
N1-C7-C6	126.870	-	127.210	126.8	127.000	-
C9-C8-N1	110.040	108.9	110.120	111.1	110.000	-
N3-C9-C8	110.480	110.9	110.590	110.7	110.600	-
C11-C10-N3	109.690	110.3	109.610	110.0	109.520	-
N4-C11-C10	109.680	109.3	109.610	105.6	109.522	-
N4-C12-C13	110.490	110.6	110.600	108.7	110.620	-
N2-C13-C12	110.040	108.6	110.240	108.8	110.008	-
N2-C14-C15	126.870	126.1	127.620	127.1	126.990	-
C20-C15-C14	122.880	123.9	122.100	123.2	122.030	-
C20-C15-C16	119.770	119.4	119.960	121.8	120.500	-
C14-C15-C16	117.330	116.7	117.910	114.9	117.440	-
C17-C16-C15	122.060	112.3	121.570	119.8	121.090	-
C16-C17-C18	118.470	118.5	119.430	121.5	119.550	-
C19-C18-C17	121.210	121.6	120.820	118.9	121.050	-
C18-C19-O3	-	-	124.790	123.0	125.530	-
C18-C19-C20	121.960	121.8	121.550	122.1	121.080	-
O3-C19-C20	-	-	113.640	114.8	113.360	-
O2-C20-C15	123.850	123.4	124.640	126.5	124.350	-
O2-C20-C19	119.510	120.2	118.910	118.0	118.840	-
C15-C20-C19	116.340	116.3	116.260	115.4	116.500	-
C7-N1-C8	118.380	119.2	118.759	119.2	118.470	-
C7-N1-Zn1	123.160	121.9	123.280	126.1	123.210	-
C8-N1-Zn1	116.960	115.4	116.390	114.1	116.580	-
C14-N2-C13	118.380	117.5	119.210	118.1	118.600	-
C14-N2-Zn1	123.150	121.7	123.070	123.5	123.080	-
C13-N2-Zn1	116.980	115.5	116.170	117.4	116.580	-

Table 4.17 (continued).

Bond Angles (°)	$ZnSal_2$trien		$ZnSal_2$(OMe)trien		$ZnSal_2$(OEt)trien	
	B3LYP/ 6-31G(d)	Exp.	B3LYP/ 6-31G(d)	Exp.	B3LYP/ 6-31G(d)	Exp.
C9-N3-C10	116.880	113.3	117.430	116.7	117.430	-
C9-N3-Zn1	103.230	107.5	103.390	104.3	104.090	-
C10-N3-Zn1	111.330	107.1	111.000	104.4	110.441	-
C11-N4-C12	116.890	113.7	117.430	115.4	117.420	-
C11-N4-Zn1	110.890	107.9	110.600	111.7	110.410	-
C12-N4-Zn1	103.990	107.4	104.070	106.6	104.090	-
C1-O1-Zn1	129.010	120.5	129.180	129.7	129.020	-
C20-O2-Zn1	128.970	121.7	129.240	128.4	129.000	-
C22-O3-C19	-	-	117.580	117.2	119.510	-
C2-O4-C21	-	-	117.580	116.4	119.500	-
O3-C22-C23	-	-	-	-	112.810	-
O4-C21-C24	-	-	-	-	112.810	-
O2-Zn1-O1	115.590	96.05	117.110	108.2	117.110	-
O2-Zn1-N1	94.860	89.80	94.870	91.11	94.790	-
O1-Zn1-N1	84.670	84.99	83.770	86.21	84.480	-
O2-Zn1-N2	84.690	83.94	83.530	86.04	84.450	-
O1-Zn1-N2	94.870	87.94	94.710	90.92	94.730	-
N1-Zn1-N2	179.150	170.0	177.020	175.1	178.520	-
O2-Zn1-N4	150.970	158.4	150.170	154.3	150.210	-
O1-Zn1-N4	88.390	94.73	87.470	90.90	87.500	-
N1-Zn1-N4	103.118	109.7	104.760	107.5	104.430	-
N2-Zn1-N4	76.450	77.83	77.960	76.43	77.030	-
O2-Zn1-N3	87.280	96.27	87.910	89.54	88.030	-
O1-Zn1-N3	151.680	159.0	150.060	156.6	150.060	-
N1-Zn1-N3	76.930	78.14	77.840	78.17	77.360	-
N2-Zn1-N3	102.980	110.21	105.460	105.7	104.820	-
N4-Zn1-N3	75.630	79.57	76.040	77.59	75.810	-

Table 4.18 Dihedral angles data for the structures of $ZnSal_2$trien, $ZnSal_2$(OMe)trien and $ZnSal_2$(OEt)trien.

Dihedral angles (°)	$ZnSal_2$trien	$ZnSal_2$(OMe)trien	$ZnSal_2$(OEt)trien
	B3LYP/6-31G(d)	B3LYP/6-31G(d)	B3LYP/6-31G(d)
C1-O1-Zn1-O2	63.975	62.639	61.533
O1-Zn1-O2-C20	64.010	62.430	61.340
C1-C6-C7-N1	-1.960	-2.140	-2.150
C6-C7-N1-C8	176.860	176.350	176.620
C7-N1-C8-C9	153.530	153.060	152.260
N1-C8-C9-N3	45.290	45.030	45.020
C8-C9-N3-C10	71.040	71.340	71.170
C9-N3-C10-C11	-158.930	-159.120	-159.390
N3-C10-C11-N4	55.270	55.220	55.810
C10-C11-N4-C12	-158.830	-159.130	-159.420
C11-N4-C12-C13	71.090	71.330	71.140
N4-C12-C13-N2	45.350	45.090	44.980
C12-C13-N2-C14	153.400	153.040	152.250
C13-N2-C14-C15	176.840	176.330	176.663
N2-C14-C15-C20	-1.950	-2.090	-2.150
O1-C1-C2-O4	-	0.000	0.840
C1-C2-O4-C21	-	178.100	178.870
C2-O4-C21-C24	-	-	81.720
O2-C20-C19-O3	-	0.000	0.880
C20-C19-O3-C22	-	178.100	178.940
C19-O3-C22-C23	-	-	81.680

CHAPTER V

CONCLUSION

$ZnSal_2$trien, $ZnSal_2$(OMe)trien, $ZnSal_2$(OEt)trien, $ZnSal_2$(di-*t*-Bu)trien, $NiSal_2$trien, $NiSal_2$(OMe)trien, $NiSal_2$(OEt)trien and $NiSal_2$(di-*t*-Bu)trien have been synthesized. Protonation constants and stability constants of Schiff base ligands and Schiff base metal complexes were determined by means of potentiometric titrations. The proton binding ability of Schiff base ligands corresponds to the electron density of each atom. This implies that all ligands can bind four protons, the first two protons bind to two phenolic groups and the last two protons bind to two amino groups. Since $ZnSal_2$(di-*t*-Bu)trien and $NiSal_2$(di-*t*-Bu)trien are very sensitive to acid. They could be hydrolyzed in acid solution and converted to starting materials and therefore the experimental data were not obtained.

Stability constants of nickel complexes are higher than those of zinc complexes which indicates that nickel complexes are more stable than zinc complexes. Since the electron configuration of nickel(II) and zinc(II) ions are $[Ar]3d^6 4s^2$ and $[Ar]3d^8 4s^2$, respectively, nickel(II) ion has more ability in forming the complexes with hexadentate Schiff base ligands than zinc(II) ion.

The stability constants of nickel complexes increase when the complexes have the electron donating groups, CH_3O- and C_2H_5O-, on the aromatic ring. This could be explained by electronic effect of substituted group on the aromatic ring. Electron density is found at ortho-para positions which have a direct effect to phenolic oxygen. As a result, the phenolic oxygen has more electrons which lead to good ability in forming metal complexes. The complex formation of $NiSal_2$(OEt)trien and $NiSal_2$(OMe)trien is better than $NiSal_2$trien which has no electron donating group.

On the other hand, stability constants of zinc complexes decrease when their complexes have CH_3O- and C_2H_5O- as substituents on the aromatic ring since electron configuration of Zn^{2+} is $[Ar]3d^{10}$. The zinc complex is thus less stable when coordinates to electron rich ligand.

The structures of Sal_2trien, $ZnSal_2$trien, Sal_2(OMe)trien, $ZnSal_2$(OMe)trien, Sal_2(OEt)trien and $ZnSal_2$(OEt)trien were optimized by Density Functional Theory (DFT) calculations using 6-31G(d) basis set. Internal energy of binding of $ZnSal_2$trien,

$ZnSal_2$(OMe)trien and $ZnSal_2$(OEt)trien complexes at B3LYP/6-31G(d) level are -736.83, -775.88 and -724.91 kcal/mol, respectively. This indicates that the order of stability of zinc complexes is $ZnSal_2$(OMe)trien > $ZnSal_2$trien > $ZnSal_2$(OEt)trien. The results from structure optimization of Sal_2trien, Sal_2(OMe)trien, Sal_2(OEt)trien and their zinc complexes at B3LYP/6-31G(d) level are that order of preorganization energy of Schiff base ligands are Sal_2(OEt)trien > Sal_2trien > Sal_2(OMe)trien, respectively. B3LYP/6-31G(d) optimized geometrical data of $ZnSal_2$trien and $ZnSal_2$(OMe)trien are in good agreement with the X-ray crystallographic data.

Suggestion for future work

From all aforementioned results and discussion, future works should be focused on:

1. $NiSal_2$trien, $NiSal_2$(OMe)trien and $NiSal_2$(OEt)trien should be studied by quantum chemical calculation to compare with zinc complexes data.
2. Stepwise protonation energy of Schiff base ligand and derivative should be optimized by Density Functional Theory (DFT).

REFERENCES

1. Garnovskii, A. D.; Nivorozhkin, A. L. and Minkin, V. I., "Ligand environment and the structure of Schiff base adducts and tetracoordinated metal-clelated", *Coord. Chem. Rev*., **1993**, *126*, 1-69.
2. Archer, R. A., "Coordination chemistry from monomers to copolymers", *Coord. Chem. Rev*., **1993**, *128*, 49-68.
3. Kaliyappan, T. and Kannan, P., "Co-ordination polymers", *Prog. Polym. Sci*., **2000**, *25*, 343-370.
4. Ziesel, R., "Schiff-based bipyridine ligands. Unusual coordination features and mesomorphic behaviour", *Coord. Chem. Rev*., **1993**, *216-217*, 195-223.
5. Costamagna, J.; Vargas, J.; Latorre, R.; Alvarado, A. and Mena, G., "Coordination compounds of copper, nickel and iron with Schiff base derived from hydroxynaphthaldehydes and salicylaldehydes", *Coord. Chem. Rev*., **1992**, *119*, 67-88.
6. Jacobsen, E. N., "Highly enantioselective epoxidation catalysts derived from 1,2-diaminocyclohexane", *J. Am. Chem. Soc*., **1991**, *113*, 7063-7064.
7. Mashhadizadeh, M. H.; Sheikhshoaie, I. and Saeid-Nia, S., "Nickel(II)-selective membrane potentiometric sensor using a recently synthesized Schiff base as neutral carrier", *Sensors*., **2003**, *94*, 241-246.
8. Chantarasiri, N.; Tuntulani, T. and Chanma, N., "Application of hexadentate Schiff base metal complexes as crosslinking agents for diglycidyl ether of bisphenol A", *Eur. Polym. J*., **2000**, *36*, 889-894.
9. Chantarasiri, N.; Chulamanee, C.; Mananunsap, T. and Muangsin, N., "Thermally stable metal-containing polyureas from hexadentate Schiff base metal complexes and diisocyanates", *Polym. Degrad. Stab*., **2004**, *86*, 505-513.

10. Martell, A. E.; Kong, D.; Motekaitis, R. J. and Reibenspies, J. H., "Two novel homodinuclear Ni(II) and Cu(II) complexes with a 24-membered octadentate hexaazamacrocyclic ligand: stability and X-ray crystal structures", *Inorg. Chim. Acta*., **2001**, *317*, 243-251.

11. Dechamps-Olivier, I.; Soibinet, M.; Mohamadou, A. and Alincourt, M., "X-ray crystal structure, ESR and potentiometric studies of copper(II) complexes with (2-pyridylmetyl, 3-pyridylmetyl amine ligand)", *Inorg. Chem. Commun*., **2004**, *7*, 405-409.

12. Lahiri, G. K.; Mondal, B.; Naumov, P. and Ng, S.W., "Crystal structure and geometry-optimization study of 2-benzyliminiometylene-4-nitrophenolate", *J. Mol. Struct*., **2002**, *613*, 131-135.

13. Gans, P.; Sabatini, A. and Vacca, A., "SUPERQUAD: an improved general program for computation of formation constants from potentiometric data", *J. Chem. Soc. Dalton Trans*.,**1985**, 1195-1199.

14. Frisch, M. J.; Trucks, G. W.; Schlegel, H. B.; Scuseria, G. E.; Robb, M. A.; Cheeseman, J. R.; Montgomery, J. A.; Jr.; Vreven, T.; Kudin, K. N.; Burant, J. C.; Millam, J. M.; Iyengar, S. S.; Tomasi, J.; Barone, V.; Mennucci, B.; Cossi, M.; Scaimani, G.; Rega, N.; Petersson, G. A.; Nakatsuji, H.; Hada, M.; Ehara, M.; Toyota, K.; Fukuda, R.; Hasegawa, J.; Ishida, M.;Nakajima, T.; Honda, Y.; Kitao, O.; Nakai, H.; Klene, M.; Li, X.; Knox, J. E.; Hratchian, H. P.; Cross, J. B.; Adamo, C.; Jaramillo, J.; Gomperts, R.; Startmann, R. E.; Yazyev, O.; Austin, A. J.; Cammi, R.; Pomelli, C.; Ochterski, J. W.; Ayala, P. Y.; Morokuma, K.; Voth, G. A.; Salvador, P.; Dannenberg, J. J.; Zakrzewski, V. G.; Dapprich, S.; Daniels, A. D.; Strain, M. C.; Farkas, O.; Malick, D. K.; Rabuck, A. D.; Raghavachari, K.; Foresman, J. B.; Ortiz, J. V.; Cui, Q.; Baboul, A. G.; Clifford, S.; Cioslowski, J.; Stefanov, B. B.; Liu, G.; Liashenko, A.; Piskorz, P.; Komaromi, I.; Martin, R. L.; Fox, D. J.; Keith, T.; Al-Laham, M.A.; Peng, C. Y.; Nanayakkara, A.; Challacombe, M.; Gill, P. M. W.; Johnson, B.; Chen, W.; Wong, M. W.; Gonzalez, C. and Pople, J. A., Gaussian 03, Revision B. 03, Gaussian, Inc., Pittsburgh PA, **2003**.

15. Schaftenaar, MOLDEN 3.8; CAOS/CAMM Center Nijmegen,Toernooiveld, Nijmegen, Netherlands, **1991**.

16. Hehre, W. J.; Steward, R. F. and Pople, J. A., “Self-Consistent Molecular-Orbital Methods. I. Use of Gaussian Expansions of Slater-Type Atomic Orbitals”, *J. Chem. Phys*., **1969**, *51*, 2657-2664.

17. Dichfield, R.; Hehre, W. J. and Pople, J. A., “Self-Consistent Molecular-Orbital Methods. IX. An Extended Gaussian-Type Basis for Molecular-Orbital Studies of Organic Molecules”, *J. Chem. Phys*., **1971**, *54*, 724-728.

18. Hehre, W. J.; Dichfield, R. and Pople, J. A., “Self—Consistent Molecular Orbital Methods. XII. Further Extensions of Gaussian—Type Basis Sets for Use in Molecular Orbital Studies of Organic Molecules”, *J. Chem. Phys*., **1972**, *56*, 2257-2261.

19. Hariharan, P. C. and Pople, J. A., “Accuracy of AH, Equilibrium Geometries by Single Determinant Molecular Orbital Theory”, *Mol. Phys*., **1974**, *27*, 209.

20. Gordon, M. S., “The isomers of silacyclopropane”, *Chem. Phys. Lett*., **1980**, *76*, 163-168.

21. Hariharan, P. C. and Pople, J. A., “The influence of polarization functions on molecular orbital hydrogenation energies”, *Theo. Chim. Acta*., **1973**, *28*, 213.

22. Dunning, T. H. and Hay, P. J., “In Modern Theoretical Chemistry”, Schaefer III, Plenum, New York, **1976**.

23. McLean, A. D. and Chandler, G. S., “Contracted Gaussian basis sets for molecular calculations. I. Second row atoms, Z=11–18”, *J. Chem. Phys*. **1980**, *72*, 5639-5648.

24. Krishman, R.; Binkley, J. S.; Seeger, R. and Pole, J. A., “Self-consistent molecular orbital methods. XX. A basis set for correlated wave functions”, *J. Chem. Phys*., **1980**, *72*, 650-654.

25. Wachter, A. H. J., “Gaussian Basis Set for Molecular Wavefunctions Containing Third-Row Atoms”, *J. Chem. Phys*., **1970**, *52*, 1033-1036.

26. Hey, P. J., “Gaussian basis sets for molecular calculations. The representation of 3d orbitals in transition-metal atoms”, *J. Chem. Phys*., **1977**, *66*, 4377-4384.

27. Raghavachari, K.; and Truck, G. W., “Highly correlated systems. Excitation energies of first row transition metals Sc–Cu”, *J. Chem. Phys*., **1989**, *91*, 1062-1065.

28. Binning, R. C. Jr. and Curtiss, L. A., “Compact contracted basis sets for third-row atoms: Ga-Kr”, *J. Comp. Chem*. **1990**, *11*, 1206-1216

29. McGrath, M. P. and Random, L., “Extension of Gaussian-1 (G1) theory to bromine-containing molecules” *J. Chem. Phys*., **1991**, *94*, 511-516.

30. Arnaud-Neu, F.; Barrett, G.; Harris, S. J.; Owens, M.; Mckervey, M. A.; Schwing-weill, M. J. and Schwinte, P., “Cation complexation by chemically modified calixarenes. 5. Protonation constants for calixarene carboxylates and stability constants of their alkali and alkaline-earth complexes”, *Inorg. Chem*., **1993**, *32*, 2644-2650.

31. Becke, A. D., “A new mixing of Hartree–Fock and local density-functional theories”, *J. Chem. Phys*., **1993**, *98*, 1372-1377.

32. Becke, A. D., “Density-functional thermochemistry. III. The role of exact exchange”, *J. Chem. Phys*., **1993**, *98*, 5648-5652.

33. Kohn, W. and Sham, L. J., “Self-consistent equations including exchange and correlation effects”, *Phys.Rev*., **1965**, *140*, A1133-A1138.

34. Foresman, J. B. and Frisch, A., “Exploring chemistry with electronic structure methods”, 2nd ed., Gaussian, Inc., Pittsburgh PA, **1993**.

35. Vosco, S. H.; Wilk, L. and Nusair, M., “Accurate spin-dependent electron liquid correlation energies for local spin density calculations: a critical analysis”, *Can. J. Phys*., **1980**, *58*, 1200.

36. Lee, C.; Yang, W. and Parr, R. G., “Development of the Colle-Salvetti correlation-energy formula into a functional of the electron density”, *Phys Rev*, **1988**, *B37*, 785-789.

37. Irving, H. and Williams, R. J. P., “Order of stability of metal complexes”, Nature (London)., **1948**, *162*, 746-747.

38. Cotton, F. A.; Wilkinson, G.; Murillo, C. A. and Bochmann, M., *Advanced Inorganic Chemistry*, Chichester: John Wiley & Sons, **1999**.

39. Chantarasiri, N.; Ruangpornvisuti, V.; Muangsin, N.; Detsen, H.; Mananunsap, T.; Batiya, C. and Chaichit, N., “Structure and physico-chemical properties of hexadentate Schiff base zinc complexes derived from salicylaldehydes and triethylenetetramine”, *J. Mol. Struct*., **2004**, *701*, 93-103.

VITAE

Mr. Hussadee Detsen was born on April 27, 1980 in Loei, Thailand. He received his Bachelor's degree of Science in Chemistry from Srinakharinwiroj University in 2001. Science 2002, he has been a graduate student studying in the field of Organic Chemistry at Chulalongkorn University and become a member of Supramolecular Chemistry Research Unit under the supervision of Associate Professor Dr. Nualphun Chantarasiri. He finished his study in Master's degree of Science in Chemistry in 2005.